

AD-A091 168

GENERAL ATRONICS CORP PHILADELPHIA PA
HARMONIC CANCELLATION SYSTEM.(U)

F/G 17/2.1

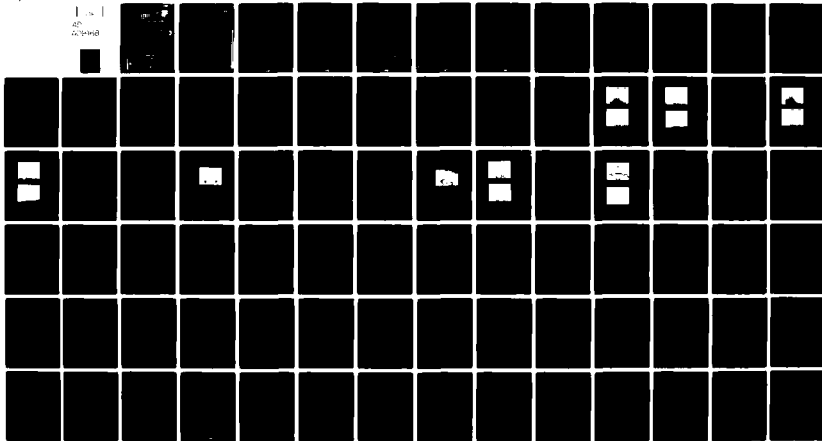
UNCLASSIFIED

SEP 80 5 J ROSASCO
GAC-3398-3385-24

RADC-TR-80-116

F30602-78-C-0191
NL

1 1
20
20-1198
■



END
DATE
FILMED
12-80
DTIC

AD A091168

RADC-TR-80-116
Final Technical Report
September 1980

LEVEL

P



HARMONIC CANCELLATION SYSTEM

General Atronics Corporation (Magnavox)

Dr. Stephen J. Rosasco

DTIC
ELECTE
NOV 3 1980
C D

APPROVED FOR PUBLIC RELEASE; DISTRIBUTION UNLIMITED

DDC FILE COPY.

ROME AIR DEVELOPMENT CENTER
Air Force Systems Command
Griffiss Air Force Base, New York 13441

8011 03 147

This document has been reviewed by the RADC Plans Division
in accordance with the National Technical Information Administration
policy and is releasable to the general public, including foreign
countries.

RADC-TR-60-116 has been reviewed and is approved for publication.

APPROVED: *Wayne E. Woodward*
WAYNE E. WOODWARD
Project Engineer

APPROVED: *David C. Luke*
DAVID C. LUKE, Lt Col, USAF
Chief, Reliability & Compatibility Division

FOR THE COMMANDER: *John P. Huss*
JOHN P. HUSS
Acting Chief, Plans Division

SUBJECT TO EXPORT CONTROL LAWS

This document contains information for manufacturing or using munitions of war. Export of the information contained herein, or release to foreign nationals within the United States, without first obtaining an export license, is a violation of the International Traffic in Arms Regulations. Such violation is subject to a penalty of up to 2 years imprisonment and a fine of \$100,000 under 22 U.S.C. 2778.

Include this notice with any reproduced portion of this document.

If your address has changed or if you wish to be removed from the RADC mailing list, or if the addressee is no longer employed by your organization, please notify RADC (RADC) Griffiss AFB NY 13441. This will assist us in maintaining a correct mailing list.

Do not return this copy. Retain or destroy.

UNCLASSIFIED

SECURITY CLASSIFICATION OF THIS PAGE (When Data Entered)

19 REPORT DOCUMENTATION PAGE		READ INSTRUCTIONS BEFORE COMPLETING FORM	
1. NUMBER RADC TR-80-116 ✓		2. GOVT ACCESSION NO. AD-A091168	3. RECIPIENT'S CATALOG NUMBER
4. TITLE (and Subtitle) HARMONIC CANCELLATION SYSTEM		5. TYPE OF REPORT & PERIOD COVERED Final Technical Report, Sep 78 - Jan 80	
7. AUTHOR(S) Dr. Stephen J. Rosasco		14) GAC	6. PERFORMING ORG. REPORT NUMBER 3398-3385-24 ✓
9. PERFORMING ORGANIZATION NAME AND ADDRESS General Atronics Corporation (Magnavox) 1200 East Mermaid Lane Philadelphia PA 19118 ✓		15) F30602-78-C-0191	8. CONTRACT OR GRANT NUMBER(S)
11. CONTROLLING OFFICE NAME AND ADDRESS Rome Air Development Center (RBCT)		16) 23380405	10. PROGRAM ELEMENT PROJECT, TASK AREA & WORK UNIT NUMBERS 62702F 23380405
14. MONITORING AGENCY NAME & ADDRESS (if different from Controlling Office) Same		17) Sep 1980	12. REPORT DATE
16. DISTRIBUTION STATEMENT (of this Report) Approved for public release: distribution unlimited.		18) 82	13. NUMBER OF PAGES
17. DISTRIBUTION STATEMENT (of the abstract entered in Block 20, if different from Report) Same		15. SECURITY CLASS. (of this report) UNCLASSIFIED	
18. SUPPLEMENTARY NOTES RADC Project Engineer: Wayne E. Woodward (RBCT)		15a. DECLASSIFICATION DOWNGRADING SCHEDULE N/A	
19. KEY WORDS (Continue on reverse side if necessary and identify by block number) Electromagnetic Compatibility Communications HF/VHF/UHF Intermodulation Products			
20. ABSTRACT (Continue on reverse side if necessary and identify by block number) The objective of this effort was to investigate Interference Cancellation System (ICS) techniques to solve the harmonic and intermodulation products (IMP) generated as the result of high power jammers, HF/VHF/UHF transmitters signals impinging on a nonlinear junction somewhere on the aircraft during flight. The problem becomes very complex when trying to receive a desired satellite starved signal. Since a reference sample of the nonlinear signal is not available, it has to be synthesized to a			

DD FORM 1 JAN 71 1473 EDITION OF 1 NOV 65 IS OBSOLETE

UNCLASSIFIED

(Cont'd)

SECURITY CLASSIFICATION OF THIS PAGE (When Data Entered)

14700

5014

UNCLASSIFIED

SECURITY CLASSIFICATION OF THIS PAGE (When Data Entered)

Item 20 (Cont'd)

high degree of accuracy in order to be able to cancel the interfering signal. The crux of this problem is the synthesization of the non-linear signal without concurrently cancelling the desired signal.

A

UNCLASSIFIED

SECURITY CLASSIFICATION OF THIS PAGE (When Data Entered)

SUMMARY

This report documents the results of a study of techniques for cancelling nonlinearity generated interference from the input of sensitive receivers. Harmonic interference is caused when a fundamental signal from a communications transmitter impinges on a nonlinearity of some type, producing harmonics which couple into the antenna of a colocated receiver tuned at a different frequency. More complex forms of interference are produced when two or more fundamental signals mix in a nonlinearity, generating intermodulation products which couple into the receiver. Means of cancelling both forms of interference by utilizing only the fundamentals have been investigated.

The study consisted of an analysis of the interference generated by a nonlinearity, laboratory experiment to verify the assumption of a memoryless nonlinearity and to evaluate the basic approach to cancellation, and a computer simulation of an harmonic interference cancellation technique. Various cancellation system configurations were developed for the cancellation of harmonic and intermodulation interferences produced by multiple nonlinearities. The laboratory experiments and computer simulations indicate that the harmonic cancellation technique appears to be realizable and practical. The report concludes with a discussion of some of the major issues that must be resolved in any practical realization.

The author acknowledges the assistance of Burton S. Abrams for some of the analytical and experimental results contained in the report.

Accession For	
NTIS GRA&I	<input checked="" type="checkbox"/>
DTIC TAB	<input type="checkbox"/>
Unannounced	<input type="checkbox"/>
Justification	
By _____	
Distribution/	
Availability Codes	
Dist	Avail and/or Special
A	

TABLE OF CONTENTS

1.0	INTRODUCTION.....	1
1.1	Background.....	2
2.0	ANALYSIS OF DISTORTION PRODUCTS.....	5
2.1	Harmonic Distortion.....	5
2.2	Intermodulation Product Distortion.....	8
2.3	Multiple Nonlinearities.....	10
3.0	EXPERIMENTAL RESULTS.....	13
3.1	Frequency Dependence of Nonlinearities.....	13
3.2	Time Domain Synthesis of Harmonic Envelope.....	17
3.3	Fourier Expansion Harmonic Synthesis.....	21
4.0	DISTORTION PRODUCT CANCELLATION SYSTEM CONFIGURATION.....	31
4.1	Harmonic Envelope Synthesis.....	31
4.1.1	Gate Function Synthesis.....	34
4.1.2	Polynomial Expansion Envelope Synthesis.....	41
4.2	Intermodulation Product Synthesis.....	43
4.2.1	Synthesis of the IMP Envelope by Use of Gate Functions.....	43
4.2.2	Polynomial Expansion IMP Envelope Synthesis.....	47
4.2.3	System Configuration for Multiple Nonlinearities.....	48
5.0	SIMULATION OF ENVELOPE SYNTHESIS BY GATE FUNCTIONS.....	51
5.1	Description of Simulation.....	51
5.2	Simulation Results.....	54
6.0	CONCLUSIONS AND RECOMMENDATIONS.....	61
	APPENDIX A: Cancellation Achievable by Different Nonlinearities.....	63
	APPENDIX B: Listing of FORTRAN Program.....	71

LIST OF ILLUSTRATIONS

1. Test Setup to Investigate Frequency Dependence of Nonlinearities...	14
2. ARC-164 Test Nonlinearity.....	15
3. ARC-164 Test Nonlinearity - Detail.....	16
4. Diode Test Nonlinearity.....	18
5. Diode Test Nonlinearity - Detail.....	19
6. Experimental Setup for Time Domain Harmonic Envelope Synthesis.....	20
7. Uncancelled ICS Output.....	22
8. Experimental Setup for Fourier Expansion Harmonic Envelope Synthesis.....	24
9. The Experimental Setup.....	26
10. Spectrum of the ICS Output.....	27
11. ICS Output Spectrum	29
12. Waveform of Synthesized Harmonic Modulation.....	29
13. Harmonic Interference Cancellation System.....	32
14. Harmonic Cancellation for Multiple Nonlinearities.....	33
15. Harmonic Synthesis	35
16. Gate Functions	37
17. Typical Gate Function Expansion.....	38
18. Harmonic Synthesis Using Gate Functions.....	40
19. Harmonic Synthesis Using Polynomials.....	42
20. IMP Cancellation System.....	44
21. Synthesis of IMP Amplitude Modulation.....	45
22. IMP Envelope Synthesis Using Gate Functions.....	46
23. IMP Envelope Synthesis Using Polynomials.....	49
24. Harmonic Envelope Synthesis Simulation.....	52
25. Synthesized I and Q Nonlinearities.....	58
A-1. Model for Cancellation Analysis.....	65

EVALUATION

Harmonics and intermodulation products (IMP) from high power HF/VHF/UHF transmitters aboard B-52, FB-111, and C-1 aircraft are interfering with the reception of a satellite starved desired UHF signal. (For example, the tenth harmonics of an HF transmitter (25 MHz) falls in the UHF range (250 MHz). Since the interfering and desired signal occupy the same frequency band, conventional filters will not solve the problem nor will conventional Interference Cancellation Systems (ICS's) solve this problem. Conventional collocated ICS's operate on the principle that a small portion of the collocated interfering transmitter signal is sampled and adjusted in amplitude and phase so that it cancels out the interfering signal arriving at the receiver input. However, in this case, the "harmonic" or "IMP" interference waveform arriving at the receiver is nonlinearly related to the one or the other, or both offending transmitters. For this case, a harmonic cancellation system is required for which no other solution is apparent.

The significance of this effort is that it has direct application to fighters, bombers, and C-1 aircraft, reference TPR R4C. In addition, this technology will have direct application to any future system wherein jammers and/or satellites communications are employed.

Wayne E. Woodward

WAYNE E. WOODWARD
Project Engineer

1.0 INTRODUCTION

The continually increasing communication requirements aboard Air Force airborne platforms of all types is creating a continually more critical electromagnetic compatibility problem. The replacement of older communications equipment with new equipment utilizing solid state components, electronically tuned filters, and wider band coverage is further complicating the compatibility problem. Higher transmit powers and new transmission waveforms, especially spread spectrum types, add to the problem. The increasing use of satellite-based communication links is surfacing new interference problems because these links typically operate with little margin.

The interference problems can generally be divided into two classes: linear and nonlinear. Linear interference problems are those where the fundamental signal from a transmitter couples into a receiver and prevents the receiver from detecting or demodulating its link signal with the required fidelity or sensitivity. Nonlinear interference problems are those where the interference coupled into the receiver is a harmonic of one transmitter or some intermodulation mix of two or more transmitted signals. The nonlinear interference is produced by one or more transmit signals impinging on a nonlinearity which is assumed to be outside the victim receiver itself.

The linear interference problem can be solved by a variety of techniques. Standard filtering approaches are by far the most widely used means of eliminating this form of interference. In addition, active interference cancellation techniques can be applied to solve those linear interference problems which cannot be solved by the application of spectral filtering. While not as mature as spectral filtering, linear interference techniques are well-known and the technology is available to solve many problems. Current activity in linear interference cancelling system technology is concerned with cancelling higher power interference, with broader bandwidths, faster response, less complexity, etc.

Currently available techniques of solving nonlinear interference problems are limited to spectrum management and the elimination of the interference producing nonlinearities. Both of these approaches are becoming increasingly difficult to apply because of the demand for more communication channels and the wider bandwidth of the channels as well as the trend towards broader band, electronically tuned communications equipment which frequently is the source of the nonlinearity. In order to provide an alternate technique for combatting nonlinear interference, the application of active cancellation concepts to nonlinear interference problems is being studied.

This report documents the results of a study of the nature of nonlinear interference from the standpoint of applying active cancellation techniques to its reduction. The study involved analytical work, experimental measurements, and computer simulations to characterize the problem and to evaluate techniques for the cancellation of

nonlinearity-generated interference. Most of the study was directed at nonlinear interference which consists of harmonics of a single fundamental, since this is less complex than the more general problems involving mixes of several transmitter waveforms. An understanding and approach to solving harmonic-type interference will lead to a solution of the more general nonlinear interference problems.

An approach to providing cancellation of harmonic interference has been developed and evaluated by computer simulation. This approach involves the synthesis of the envelope of the harmonic interference by processing the fundamental envelope and the received harmonic envelope. The synthesized envelope is used to modulate a carrier at the harmonic frequency which is then used to effect cancellation of the received harmonic interference.

The canceller system is implemented by utilizing standard canceller techniques plus harmonic synthesis processing consisting of straightforward digital and analog signal processing components. It is recommended that an experimental model of this equipment be developed in order to further evaluate the capabilities of such techniques.

1.1 BACKGROUND

The identification, evaluation and elimination of nonlinearities on board Air Force aircraft is addressed in detail in reference [1]. As described in [1], a series of measurements were made on several aircraft. The measurements indicated that the predominant harmonic interferences were not produced by airframe effects ("rusty bolts," mechanical joints, etc.) as initially expected, but by nonlinearities in the communication and navigation systems.

Further tests and measurements located some of the most troublesome causes of these nonlinearities and the relative magnitude of the distortion produced by these sources. Equipment modifications to reduce the production of distortion products were investigated, implemented, and evaluated.

Subsequent measurements of the AFSATCOM receiver have indicated that additional nonlinearities are present which produce distortion products which fall in the satellite downlink band, thereby limiting the sensitivity of the receiver. This loss of sensitivity is particularly critical for satellite links such as AFSATCOM or the Global Positioning System (NAVSTAR) since these links are usually operated with little margin. Aircraft on which distortion product interference is causing problems are the EC-135C, RC-135, FB-111A, and B-52H. References [2], [3], and [4] contain descriptions of other studies which analyzed nonlinearities and means of locating them on structures as large and complicated as Navy ships. The general problem of analysis of nonlinear effects has been

[1] "Nonlinear Interference Cancellation System," RADC-TR-78-225, November 1978.

addressed by researchers in various fields for many years. The early work of Wiener as well as the later work [5] represents some of the earliest efforts to apply the tools of mathematical analysis to the solution of nonlinearity problems in engineering. Much of the analysis can be divided into consideration of two basic types of nonlinear systems: those with no memory and those containing memory. Memoryless systems (both linear and nonlinear) have the property that the system output at each instant of time is determined by the input at that instant and is unaffected by the past inputs to the system.

Much of the earlier applied work was restricted to the analysis of memoryless types of nonlinearities. More recent efforts have extended the earlier work to include nonlinearities with memory. Analysis of these more complicated nonlinearities requires more powerful analytical tools. Recently, there has been renewed interest in the solution of these problems by application of Volterra functional series. Reference 6 contains a description of this series and its application to nonlinear analysis and is typical of current applications of Volterra analysis.

Most work reported to date involves the analysis of the distortion characteristics of devices and the computation of the levels of distortion products (DP) produced by these devices or the exact fundamental waveforms in the nonlinearity. Usually, the analysis of the distortion characteristics of these devices is conducted for CW signals and, therefore, is not directly applicable to the problem of a more complex modulated carrier. No work is reported that applies directly to the problem of cancelling DP's at harmonic or intermodulation products produced by nonlinear devices excited by one or two incident signals.

- [2] Higa, Walter H., "Spurious Signals Generated by Electron Tunneling on Large Reflector Antennas," Proc IEEE, vol. 74, no. 2, February 1975.
- [3] Chase, W.N., J.W. Rockway and G.C. Salisbury, "A Method of Detecting Significant Sources of Intermodulation Interference," IEEE Trans on Electromagnetic Compatibility, vol. EMC-17, no. 2, May 1975.
- [4] Chase, W.N., "Ship RFI Survey Procedure for HF Frequencies," NELC Technical Document 336, 21 June 1974.
- [5] Wiener, N. Nonlinear Problems in Random Theory, MIT Press, 1958.
- [6] "Nonlinearity System Modelling and Analysis with Application to Communication Receivers," RADC TR-73-178, June 1978.
- [7] Thomas, E.J., "An Adaptive Echo Canceller in a Nonideal Environment (Nonlinear or Time Variant)," BSTJ, vol. 50, no. 8, October 1971.
- [8] Falconer, D.D., "Adaptive Equalization of Channel Nonlinearities in QAM Data Transmission Systems," BSTJ, vol. 57, no. 7, September 1978.

Some work is underway to provide equalization for the nonlinear characteristics of telephone channels. References [7] and [8] report on the application of these techniques to baseband equalization of telephone line nonlinearities. The work reported in reference [8] compensated for quadratic and cubic nonlinearities

(amplitude only) with a resulting improvement in the bit error rate performance of the channel. Reference [7] is a mathematical analysis and simulation of the performance of an equalizer when confronted with nonlinear distortion produced by phase jitter caused by local oscillator frequency instability in the transmission channel.

The approaches to DP cancellation considered during this study assume that the nonlinearities to be encountered in practice are memoryless and continuous with no hysteresis or jump characteristics. Laboratory measurements appear to support the truth of these assumptions. Typical communication system components such as diodes, amplifiers, mixers and electronically tuned radio front ends have been used in the experiment. The measurements made indicate that, at least over the bandwidth of interest (tens of kilohertz), the nonlinearly generated harmonic products are independent of frequency, implying that the nonlinearities have sufficiently small memory effects that they can be regarded as memoryless. It is likely that as larger frequency bands are considered (large percentage), memory effects would become more significant.

It should be emphasized that the lack of memory effects described above refers to narrow bands centered around a particular harmonic or intermodulation product carrier frequency and does not refer to wide bands spanning the radio frequency difference between the various harmonics. Therefore, mathematically, these nonlinearities are not strictly memoryless. This distinction will be addressed again later.

2.0 ANALYSIS OF DISTORTION PRODUCTS

In this section the harmonic and intermodulation product signals generated when one or more modulated fundamental carrier signals are incident on a nonlinearity are analytically investigated. In addition, the effects of multiple nonlinearities are investigated. As mentioned earlier, the analysis assumes that the nonlinearities are memoryless, continuous and single-valued. This assumption appears to be justified based on measurements of the nonlinearity characteristics of typical communications equipment and components. Section 3 contains a summary of these measurements.

The distortion product analysis is divided into three sections. First, harmonics of a single fundamental signal impinging on a nonlinearity are considered. Next, the intermodulation distortion products produced when two signals combine on a nonlinearity are analyzed. Finally, the effects of multiple nonlinearities on the characteristics of the total LP interference encountered by a receiver are analyzed.

2.1 HARMONIC DISTORTION

Modelling nonlinearities as continuous, single-valued and memoryless allows the output of a nonlinearity to be expressed as a power series expansion of the incident fundamental signal. The output of such a nonlinearity is given by

$$v_0(t) = \sum_{k=0}^{\infty} a_k v_1^k(t) \quad (2-1)$$

where $v_1(t)$ is the incident fundamental signal. The characteristics of a particular device are contained in the set of coefficients a_k . The memoryless nature of a device characterized by an expression such as (2-1) is apparent since the output at any time depends only on the input at that time and is independent of the past history of the input. For the same reason, a device whose behavior is described by (2-1) cannot display any hysteresis.

The fundamental signal incident on the nonlinearity will be represented by

$$v_1(t) = V(t) \cos(\omega_0 t + \phi(t)) \quad (2-2)$$

This representation includes amplitude and phase modulated carriers of various types, depending on the selection of the amplitude function $V(t)$ and the phase function $\phi(t)$. Inserting (2-2) in (2-1) yields

$$v_0(t) = \sum_{k=0}^{\infty} a_k V^k(t) \cos^k(\omega_0 t + \phi(t)) \quad (2-3)$$

Terms in this sum may be expanded using the results in [9] to give

$$v^k(t) \cos^k(\omega_0 t + \phi) = v^k(t) \sum_{m=0}^{\infty} 2C(k,m) \cos(m\omega_0 t + m\phi) \quad (2-4)$$

m even if k even
m odd if k odd

where

$$C(k,m) = \frac{\epsilon_m \Gamma(k+1)}{2^{k+1} \Gamma(1 - \frac{m-k}{2}) \Gamma(1 + \frac{m+k}{2})}$$

with

$$\epsilon_m = 1 \quad \text{for } m = 0$$

$$= 2 \quad \text{for } m > 0$$

$\Gamma(k)$ - Gamma function
 $= (k-1)!$ for integer, $k, k > 0$.

By utilizing the properties of the Gamma function, it can be shown that

$$c(k,m) = 0 \quad \text{for } m > k.$$

Using (2-4) in (2-3) allows the output of the nonlinearity to be expressed as

$$v_0(t) = 2 \sum_{k=0}^{\infty} a_k v^k(t) \sum_{\substack{m=0 \\ (k-m) \text{ even}}}^k C(k,m) \cos(m\omega_0 t + m\phi) \quad (2-5)$$

or by interchanging summations as

$$v_0(t) = 2 \sum_{m=0}^{\infty} \cos(m\omega_0 t + m\phi) \sum_{\substack{k=m \\ (k-m) \text{ even}}}^{\infty} a_k v^k(t) C(k,m) \quad (2-6)$$

Each of the above representations displays the structure of the harmonic distortion products in a different way. Equation (2-5) shows that each term in the power series expansion of the nonlinearity develops a sum of carriers at (alternate) harmonics of the fundamental frequency and that the fundamental phase term $\phi(t)$ is scaled by the harmonic number. All these terms are amplitude modulated by $v^k(t)$. For example, for the $k=9$ term, the following components are present:

[9] Davenport, W.B., Root, W.L., An Introduction to the Theory of Random Signals and Noise, McGraw-Hill Book Co., New York, 1978, p. 284.

$$V^9(t) \{ C(9,1) \cos(\omega_0 t + \phi) + C(9,3) \cos(3\omega_0 t + 3\phi) + C(9,5) \cos(5\omega_0 t + 5\phi) \\ + C(9,7) \cos(7\omega_0 t + 7\phi) + C(9,9) \cos(9\omega_0 t + 9\phi) \} \quad (2-7)$$

This representation shows which harmonic carriers are amplitude modulated by $V^9(t)$. The alternate representation of (2-6), on the other hand, identifies the signal structure at each harmonic. This can be seen by considering the second sum in (2-6) for a particular m . This sum, which is a combination of powers of $V(t)$, amplitude modulates the m -th harmonic carrier. The bandwidth of the modulation of the m -th harmonic is determined by the bandwidth of the fundamental modulation $V(t)$ and resulting bandwidth of the powers of $V(t)$ in the sum. The energy in these higher power terms diminishes rapidly as k increases because of the high order. Thus the bandwidth of the m -th harmonic energy is concentrated about the m -th harmonic carrier frequency. For the fundamental carrier frequencies under consideration here (2 Mhz or higher), there typically is no overlap of energy between adjacent harmonics.

Equation (2-6) clearly shows the structure of these harmonics. Generally a narrowband receiver is tuned to receive only one of these harmonics. The harmonic interference at the n -th harmonic is given by

$$v_n(t) = V_n(t) \cos(n\omega_0 t + n\phi(t)) \quad (2-8)$$

where the amplitude modulation $V_n(t)$ is

$$V_n(t) = 2 \sum_{\substack{k=n \\ (k-n) \text{ even}}}^{\infty} a_k C(k,n) V^k(t)$$

As (2-8) shows, the amplitude modulation of the n -th harmonic carrier is a sum of alternate powers of the fundamental modulation $V(t)$, beginning with the n -th power. The terms in the sum are weighted by the nonlinearity coefficients a_k and the expansion coefficients $C(k,n)$. As described above, the bandwidth of the sidebands at the n -th harmonic is determined by the fundamental modulation spectrum and the coefficients a_k and $c(k,n)$. In principle, this bandwidth is infinite, as shown by the k expansion in (2-8) for $V_n(t)$. However, the energy near the band edges of $V^k(t)$ diminishes rapidly for large k since the spectrum of $V^k(t)$ is the k -fold convolution of the spectrum of $V(t)$. In general, the dominant term in the sum is the $k=n$ term, since higher powers of $V(t)$ will be smaller in magnitude.

2.2 INTERMODULATION PRODUCT DISTORTION

In this section the analysis of the distortion products produced by a memoryless nonlinearity is extended to the case where two amplitude modulated fundamentals are incident on the nonlinearity. The output of the nonlinearity is given by (2-1) where now the input is given by

$$v(t) = A_1(t)\cos\omega_1 t + A_2(t)\cos\omega_2 t \quad (2-9)$$

in which $A_1(t)$ and $A_2(t)$ are amplitude modulations for carriers at frequencies f_1 and f_2 . For simplicity only amplitude modulation is considered. Inserting (2-9) in (2-1) yields

$$\begin{aligned} v_0(t) &= \sum_{n=0}^{\infty} a_n [A_1 \cos\omega_1 t + A_2 \cos\omega_2 t]^n \\ &= \sum_{n=0}^{\infty} a_n \sum_{i=0}^n \binom{n}{i} A_1^i A_2^{n-i} \cos^i \omega_1 t \cos^{n-i} \omega_2 t \end{aligned} \quad (2-10)$$

where the dependence of A_1 and A_2 on t has been dropped for convenience and

$$\binom{k}{i} = \frac{k!}{i!(k-i)!}$$

are the binomial coefficients.

In order to show the intermodulation frequencies explicitly, (2-10) will be expanded further by use of the following [10]:

$$\cos^n \theta = \frac{1}{2^n} \sum_{j=0}^n \binom{n}{j} \cos(n-2j)\theta$$

Using this in (2-10) results in

[10] Jolley, B.W., Summation of Series, Dover Press, 1961.

$$\begin{aligned}
v_0(t) &= \sum_{n=0}^{\infty} \sum_{i=0}^n \sum_{j=0}^i \sum_{k=0}^{n-i} \frac{a_n}{2^{n-i}} \binom{n}{i} \binom{n-i}{k} A_1^i(t) A_2^{n-i}(t) \cos((i-2j)\omega_1 t) \cos((n-i-2k)\omega_2 t) \\
&= \sum_{n=0}^{\infty} \sum_{i=0}^n \sum_{j=0}^i \sum_{k=0}^{n-i} \frac{a_n}{2^{n+1}} \binom{n}{i} \binom{n-i}{k} A_1^i(t) A_2^{n-i}(t) \{ \cos[(i-2j)\omega_1 t + \\
&\quad + (n-i-2k)\omega_2 t] + \cos[(i-2j)\omega_1 t - (n-i-2k)\omega_2 t] \} \quad (2-11)
\end{aligned}$$

which shows that the intermodulation products generated by the nonlinearity occur at frequencies

$$f_1 = m_1 f_1 \pm m_2 f_2$$

where from (2-11)

$$m_1 = i-2j$$

$$m_2 = n-i-2k$$

In general, m_1 and m_2 range over the set of positive and negative integers as can be seen by examination of the limits in (2-11). The order of the intermodulation product (IMP) is

$$\text{IMP order} = |m_1| + |m_2|$$

Since we are considering IMP interference to a narrowband receiver tuned to a frequency f_R , it is not necessary to retain all the terms in (2-11). Only those IMP which occur at f_R will get through the receiver passband. Furthermore, if we assume that the modulation sidebands of the IMP fall off rapidly so that there is no appreciable spectral overlap between the IMP, only those IMP occurring at f_R will affect the receiver. Thus, the IMP interference at f_R is given by those terms in (2-11) for which

$$f_R = m_1 f_1 + m_2 f_2.$$

There are multiple solutions for Equation (2-13), that is, sets of (m_{1i}, m_{2i}) for $i = 1, 2, \dots$ which yield the IMP at f_R . However, the IMP which causes the greatest interference are those where the order of the IMP is low, typically 3, 5, or 7. Therefore, for a particular f_R and fixed f_1 and f_2 , the values of m_1 and m_2 in (2-13) which cause the interference can be considered as unique and will be such as to provide a low order IMP. Hence, we may consider m_1 and m_2 as fixed and apply the definitions of (2-12) to reduce (2-11) to that IMP which occurs at f_R .

Making the substitution $m_1 = i+2j$ and $m_2 = n-i-2k$ eliminates the sums over k and j in (2-11) and yields the IMP at f_R as

$$v_R(t) = \sum_{\substack{n=m_1+m_2 \\ n-m_1-m_2 \\ \text{even}}}^{\infty} \sum_{\substack{i=m_1 \\ i-m_1 \\ \text{even}}}^{n-m_2} \frac{a_n}{2^{n+1}} \binom{n}{i} \binom{i}{i-m_1} \binom{n-i}{n-i-m_2} A_1^i A_2^{n-i} \cdot \cos[m_1 \omega_1 t + m_2 \omega_2 t] \quad (2-14)$$

where only the $m_1 f_1 + m_2 f_2$ term has been retained from (2-11). By transforming the summation indices using

$$l_1 = i - m_1$$

$$l_2 = n - i - m_2$$

(2-14) becomes

$$v_R(t) = \sum_{\substack{l_1=0 \\ l_1 \text{ even}}}^{\infty} \sum_{\substack{l_2=0 \\ l_2 \text{ even}}}^{\infty} \frac{a_{l_1+m_1+l_2+m_2}}{2^{l_1+m_1+l_2+m_2+1}} \frac{(l_1+m_1+l_2+m_2)! A_1^{l_1+m_1} A_2^{l_2+m_2}}{\left(\frac{l_1}{2}\right)! \left(\frac{l_1+m_1}{2}\right)! \left(\frac{l_2}{2}\right)! \left(\frac{l_2+m_2}{2}\right)!} \cos[m_1 \omega_1 t + m_2 \omega_2 t]$$

The INP at f_R can be expressed as

$$v_R(t) = y(t) \cos[(m_1 \omega_1 + m_2 \omega_2)t] \quad (2-15)$$

with

$$y(t) = \sum_{\substack{l_1=0 \\ l_1 \text{ even}}}^{\infty} \sum_{\substack{l_2=0 \\ l_2 \text{ even}}}^{\infty} c_{l_1, l_2} A_1^{l_1+m_1} A_2^{l_2+m_2} (t)$$

where the constants c_{l_1, l_2} include the expansion coefficients and the nonlinearity coefficients and are given by

$$c_{l_1, l_2} = \frac{a_{l_1+m_1+l_2+m_2}}{2^{l_1+m_1+l_2+m_2+1}} \frac{(l_1+m_1+l_2+m_2)!}{\left(\frac{l_1}{2}\right)! \left(\frac{l_1+m_1}{2}\right)! \left(\frac{l_2}{2}\right)! \left(\frac{l_2+m_2}{2}\right)!}$$

2.3 MULTIPLE NONLINEARITIES

The underlying assumption for the previous developments is that the nonlinearity generating the interference is strictly memoryless. Nonlinear devices that exhibit AM-PM conversion are not memoryless, for it takes memory to vary the zero crossings of the output waveform from those

of the input. Such an effect can be produced by a nonlinear device as simple as a diode with a capacitor across the junction, so that the R-C time constant depends on the input amplitude. More importantly, as will be shown, interference produced by a composite nonlinearity that is formed by a group of memoryless nonlinearities whose waveforms are combined with different phase shifts (e.g., due to different propagation delays) also exhibits AM-PM conversion.

As a practical matter, nonlinearities are likely to occur in multiples due to the presence of multiple communication systems on board a single aircraft. In addition, it is likely that a single communications terminal (including antenna, tuner, one or more receivers or transmitters) will contain several nonlinearities. Such a composite nonlinearity consists of individual nonlinearities radiating harmonic energy that is received by an antenna on the aircraft with slightly different propagation delays. This model is called weakly dispersive because it is assumed that the envelope delays are insignificant, but the effect on carrier phase is not. Thus, a sum of harmonic waveforms is received which constitutes the total harmonic interference that may be expressed as

$$v_n(t) = \sum_i A_i(t) \cos[n\omega_c t + n\phi(t) + \theta_i] \quad (2-16)$$

where $A_i(t)$ is the harmonic amplitude modulation associated with each nonlinearity. Each term in the sum of (2-16) corresponds to an harmonic interference as derived earlier and expressed in (2-8). The summation variable i is used to index each of the contributing nonlinearities. The phase shift θ_i , representing the effect of propagation delay, is subscripted by i the summation index i to show that, in general, its value is different for each value of i . Since the nonlinearities may vary greatly in their particular characteristics and in the amplitudes of their input fundamental waveforms, the envelopes $A_i(t)$ will also differ for different values of i .

Thus, the total n -th harmonic can be expressed as

$$v_n(t) = \left[\sum_i A_i(t) \cos\theta_i \right] \cos[n\omega_c t + n\phi(t)] - \left[\sum_i A_i(t) \sin\theta_i \right] \sin[n\omega_c t + n\phi(t)] \quad (2-17)$$

in which the inphase and quadrature components are evident. This can be made more apparent by writing

$$v_n(t) = A_I(t) \cos[n\omega_c t + n\phi(t)] + A_Q(t) \sin[n\omega_c t + n\phi(t)] \quad (2-18)$$

where

$$A_I(t) = \sum_i A_i(t) \cos\theta_i$$

$$A_Q(t) = -\sum_i A_i(t) \sin\theta_i$$

Thus it can be seen that multiple nonlinearities produce AM to PM conversion which must be accommodated in any system attempting to effect harmonic cancellation. The AM-to-PM conversion is evident by rewriting $v_n(t)$ once more as

$$v_n(t) = A(t) \cos[n\omega_c t + n\phi(t) + \theta(t)] \quad (2-19)$$

where the envelope $A(t)$ is

$$A(t) = \left(A_I^2(t) + A_Q^2(t) \right)^{1/2}$$

and the phase $\theta(t)$ is

$$\theta(t) = \tan^{-1} \left\{ \frac{A_I(t)}{A_Q(t)} \right\}$$

3 0 EXPERIMENTAL RESULTS

3.1 FREQUENCY DEPENDENCE OF NONLINEARITIES

The analysis of nonlinearity-generated interference of either the harmonic or intermodulation product type is greatly simplified if the nonlinearity in question is memoryless. Likewise the structure and complexity of a harmonic distortion cancellation system is greatly reduced if the nonlinearity is memoryless. The nonlinearity models used in Section 2 assumed that there are no memory effects present in the nonlinearity and, as a consequence of this assumption, the entire harmonic spectrum displayed no memory effects at all. In practice this is unlikely to be true. However, all that is really needed is that memory effects be negligibly small over a frequency band commensurate with the bandwidth of the modulation sidebands of the harmonic of interest. Lack of memory over a band of this extent is more likely to be found with real nonlinearities and implies that the amplitude of the modulation sidebands are not a function of the fundamental modulation frequency.

In order to experimentally evaluate these effects, two nonlinearities were tested in the laboratory to determine if their harmonic responses to an AM waveform were dependent on the frequency of the fundamental modulation. A block diagram of the test setup is given in Figure 1.

A sinusoidally modulated AM double-sideband, suppressed carrier waveform was synthesized by summing two sinusoids at equal levels with a slight frequency difference Δ , with both frequencies set near 25 MHz. The sum was amplified and lowpass filtered for harmonic rejection. The resulting waveform was then applied to the test nonlinearity, and the sixth harmonic at 150 MHz was monitored on a spectrum analyzer. Two test nonlinearities were used: an FD100 Schottky diode and the antenna port of an ARC-164 radio with its power off. The attenuator preceding the nonlinearity was adjusted to obtain approximately equal sixth harmonic power levels for both nonlinearities.

Both the ARC-164 and the diode sixth harmonic response were observed with approximately 1 kHz and 10 kHz tone spacing (at the fundamental frequency). Figure 2 is a photograph of the spectrum analyzer display with the ARC-164 used as the test nonlinearity. The upper photograph is for a 1 kHz spacing between the two fundamental tones (i.e., 25.000 MHz and 25.001 Mhz) while the lower photograph is for a 10 kHz spacing between the two fundamental tones (25.000 MHz and 25.010 Mhz). Figure 3 is for the same conditions with the analyzer vertical sensitivity improved to 2 dB/div. Comparison of the upper and lower analyzer photographs shows that there is no discernible difference between the relative sideband levels, indicating that the harmonic sideband structure is not dependent on the frequency of the fundamental modulation. The measurement technique, instrument accuracy and sensitivity permits measurement of differences in sideband levels as small as 0.5 or 0.25 dB, indicating that the ARC-164 front end (unpowered) is memoryless over a band

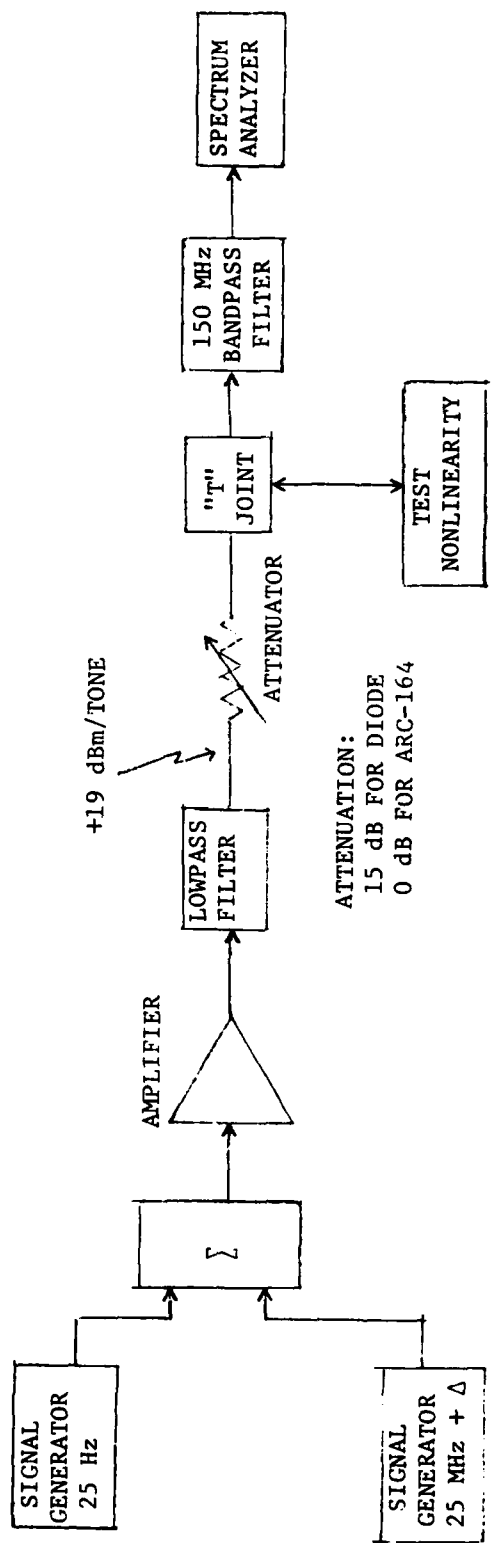
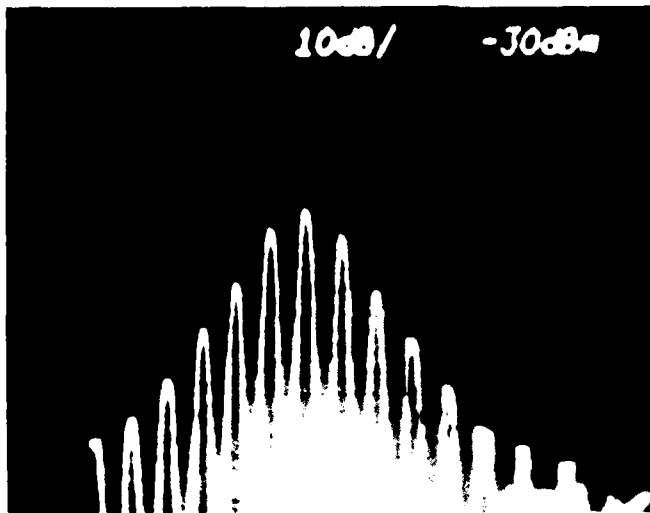
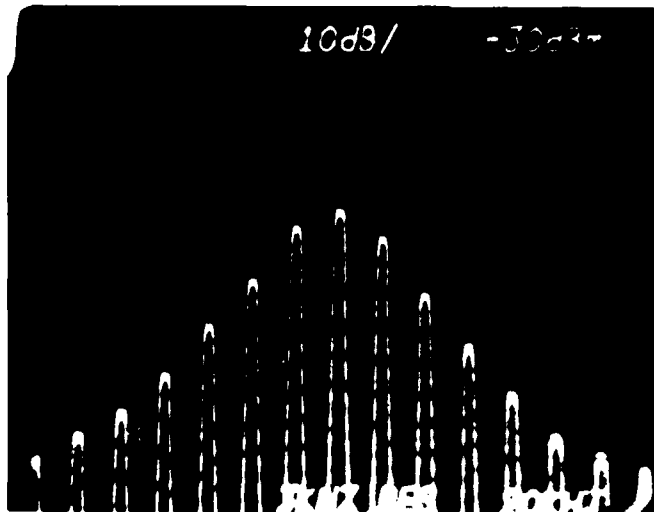


FIGURE 1. TEST SETUP TO INVESTIGATE FREQUENCY DEPENDENCE OF NONLINEARITIES



1 kHz FUNDAMENTAL
TONE SPACING

VERTICAL: 10 dB/DIV
HORIZONTAL: 2 kHz/DIV



10 kHz FUNDAMENTAL
TONE SPACING

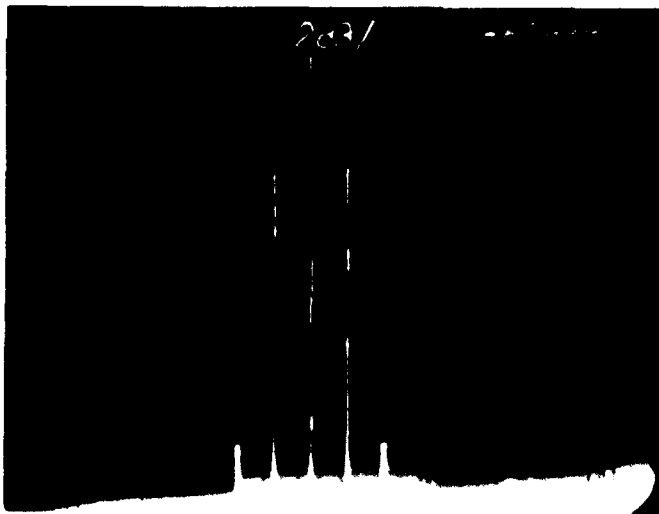
VERTICAL: 10 dB/DIV
HORIZONTAL: 20 kHz/DIV

FIGURE 2
ARC-164 TEST NONLINEARITY



1 kHz FUNDAMENTAL
TONE SPACING

VERTICAL: 2 dB/DIV
HORIZONTAL: 2 kHz/DIV



10 kHz FUNDAMENTAL
TONE SPACING

VERTICAL: 2 dB/DIV
HORIZONTAL: 20 kHz/DIV

FIGURE 3

ARC-164 TEST NONLINEARITY - DETAIL

tent of kilohertz wide to at least 0.5 to 0.25 db.

Figures 4 and 5 show the same sequence of analyzer photographs with the diode used as the test nonlinearity. The same comparison can be made showing that diode is also memoryless over the band measured.

By comparing Figure 2 to Figure 4 it can be seen that the sideband structure of the ARC-164 nonlinearity and the diode nonlinearity are different. For example, comparison of the lower photographs in each figure indicates that the ARC-164 sidebands fall off more rapidly than those of the diode. This difference in relative sideband structure means that the sixth harmonic waveform from the diode could not be used to achieve significant cancellation of interference produced by an ARC-164 front end.

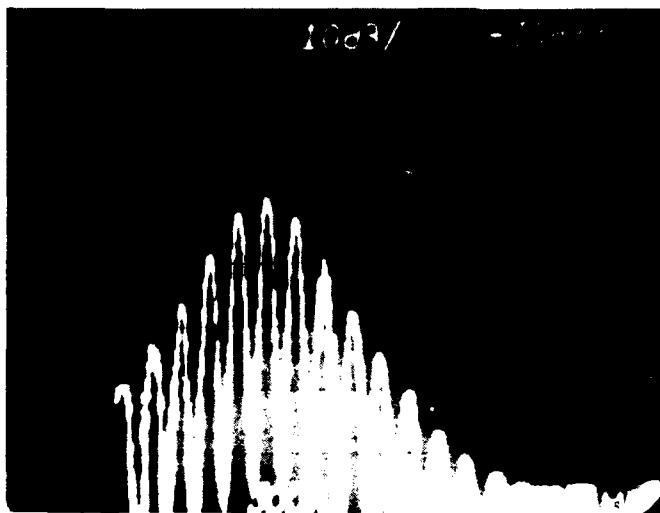
Appendix A analyzes the cancellation that can be achieved by using the harmonic distortion produced by one nonlinearity to cancel the harmonic distortion produced by a second nonlinearity.

3.2 TIME DOMAIN SYNTHESIS OF HARMONIC ENVELOPE

In order to evaluate the concept of harmonic cancellation by synthesis of the harmonic envelope, a laboratory experiment was conducted using standard laboratory equipment and an interference cancellation system. Basically, the experiment consists of generating a sinusoidally amplitude modulated fundamental which excited a nonlinearity to generate a third harmonic interference. Direct synthesis of the envelope of a third harmonic signal to effect cancellation of the interference was used. The synthesis of the third harmonic envelope was accomplished by use of a Wavetek waveform generator, the output of which was used to amplitude modulate a carrier at the third harmonic. Cancellation was accomplished by use of the MX-500, a UHF cancellation system with adaptive control loops which is capable of providing 60 dB of cancellation.

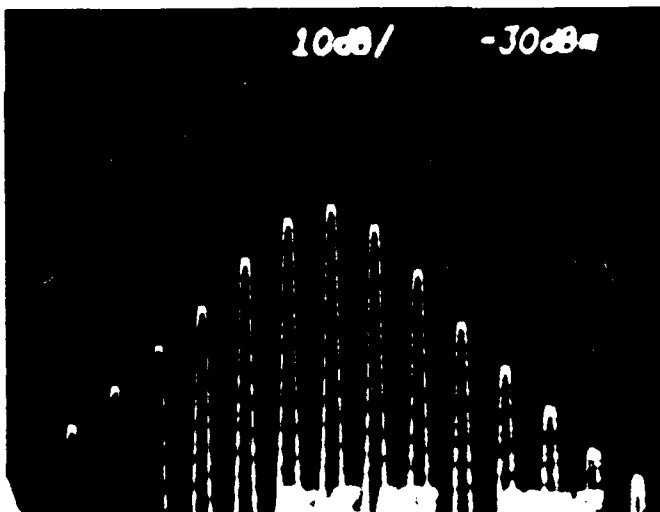
The waveform synthesizer used was a Wavetek Model No. 175, Arbitrary Waveform Generator (ARB). This generator can synthesize an approximation to any periodic waveform. It subdivides the period into N time segments, where N is selectable between 1 and 1024. The operator programs into the instrument's memory the amplitude of the waveform (quantized to 255 levels) for each time segment, by keyboard entries. The amplitude scale factor and the waveform period are also operator selectable. The generator can generate a stepwise approximation to a desired waveform, or it can be operated with smoothing between the time slots to generate a piecewise linear approximation to a desired waveform.

The experimental setup is shown in Figure 6, in which the ARB is used to amplitude modulate the third harmonic carrier as the Reference (weighted) input to an UHF interference cancellation system (ICS). The ICS Main (unweighted) input was the third harmonic from a test nonlinearity to which the amplitude-modulated fundamental was applied. The AM on the fundamental interference was sinusoidal, with the same period as that



1 kHz FUNDAMENTAL
TONE SPACING

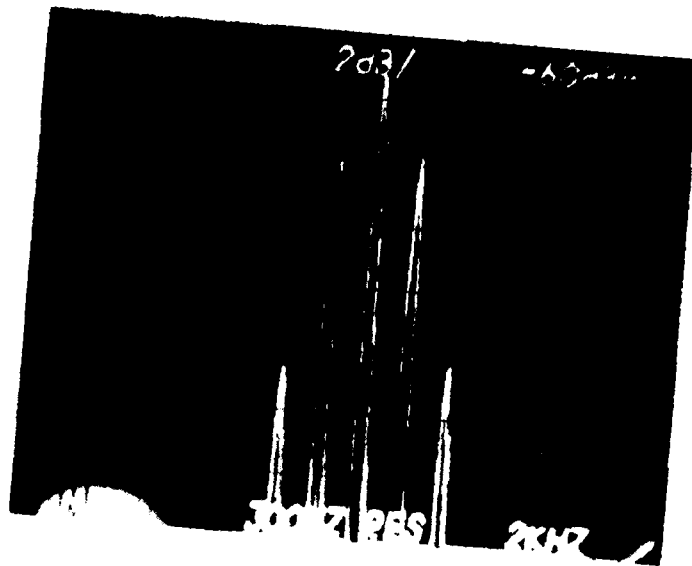
VERTICAL: 10 dB/DIV
HORIZONTAL: 2 kHz/DIV



10 kHz FUNDAMENTAL
TONE SPACING

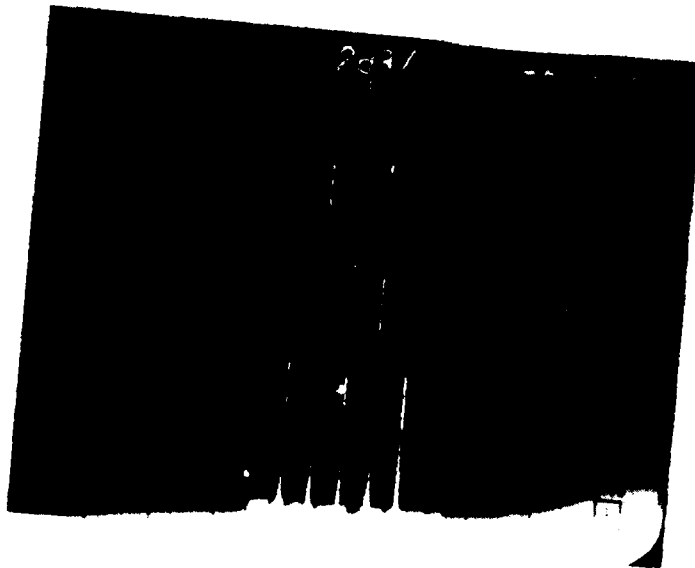
VERTICAL: 10 dB/DIV
HORIZONTAL: 20 kHz/DIV

FIGURE 4
DIODE TEST NONLINEARITY



1 kHz FUNDAMENTAL
TONE SPACING

VERTICAL: 2 dB/DIV
HORIZONTAL: 2 kHz/DIV



10 kHz FUNDAMENTAL
TONE SPACING

VERTICAL: 2 dB/DIV
HORIZONTAL: 20 kHz/DIV

FIGURE 5
DIODE TEST NONLINEARITY - DETAIL

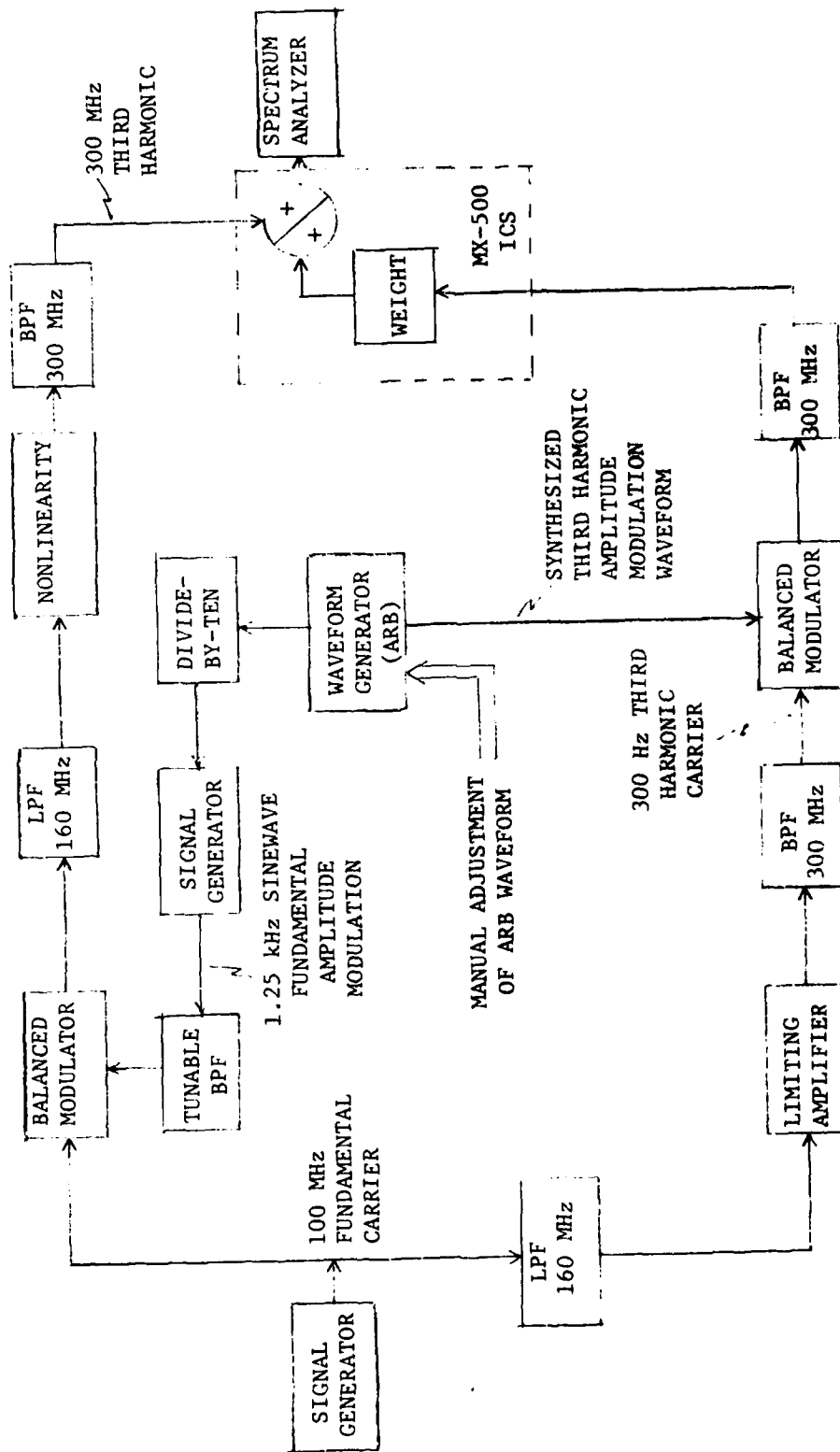


FIGURE 6. EXPERIMENTAL SETUP FOR TIME DOMAIN HARMONIC ENVELOPE SYNTHESIS

generated by the ARB. This was accomplished by using a Wavetek #171 Synthesized Signal Generator with an external 1 MHz clock provided by the 10 MHz clock of the ARB through a divide-by-ten counter. The phase of the sinusoid was adjusted by passing it through the tunable Krohn-Hite #310-AB Bandpass Filter.

The ARB was operated with a period of 1.25 kHz, subdivided into N=40 time slots. The ICS output was monitored on the spectrum analyzer used as a fixed-tuned (at 300 MHz) detector with 300 kHz IF bandwidth. The spectrum analyzer then provided a time domain display of the ICS output; its sweep was triggered from the ARB. The ARB waveform was then manually programmed point-by-point to minimize the ICS output as seen on the analyzer. The time slot modified at each iteration was the one for which the ICS output was largest. Smoothing was enabled on the ARB.

Figure 7 shows the spectrum analyzer display of the ICS output with no cancellation applied, that is, the ICS output with only the output of the test linearity connected to the ICS. Recall that the analyzer is used as a fixed tuned receiver with the horizontal axis proportional to time in this experimental setup.

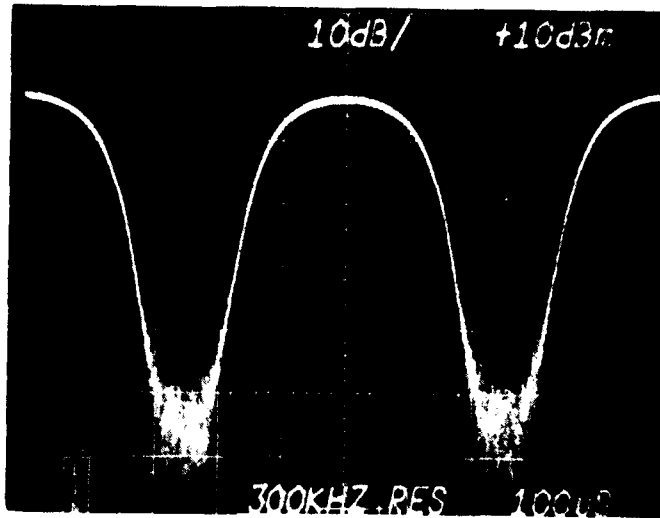
Modification of the ARB waveform point-by-point as described above allowed the peak value of the ICS output to be reduced by 20 dB. Further output minimization could not be accomplished because of an ARB malfunction in which it would, at random times, dump its memory. Further experimentation with this equipment was aborted because of this malfunction, so that more illustrative and/or precise data are not available.

It was noted that the ARB waveform needed for 20 dB of cancellation was not strictly symmetrical about its positive and negative peaks. This indicates that AM-PM conversion effects were present, further borne out by the asymmetry of the spectrum at the ICS output. This is very likely the result of the fact that other nonlinearities were present in the experimental setup (thus producing the AM-PM conversion effects described earlier in Section 2.3). When the test nonlinearity was removed, the third harmonic interference decreased by about 15 dB, indicating that other sources of distortion were present.

Although this laboratory experiment did not yield definitive data, it did demonstrate that harmonic cancellation by synthesis of the harmonic envelope is a viable concept.

3.3 FOURIER EXPANSION HARMONIC SYNTHESIS

An additional experiment was conducted to further evaluate the concept of harmonic cancellation by synthesis of the harmonic envelope. In this experiment a sinusoidal fundamental envelope was used and the harmonic envelope was synthesized as the sum of amplitude weighted and phase shifted harmonics of the fundamental. This harmonic envelope synthesis approach relies on the fact that the harmonic envelope is a sum of powers of the



Vertical Scale: 10 dB/div
Horizontal Scale: 100 μ s/div

Analyzer tuned to 300 MHz
IF Bandwidth: 300 kHz

FIGURE 7

UNCANCELLED ICS OUTPUT

fundamental envelope as shown by Equation (2-8). The synthesized harmonic envelope used in the experiment is

$$V_n(t) = \sum_{k=0}^7 A_k \cos(2\pi kft + \theta_k) \quad (3-1)$$

while the amplitude modulation of the fundamental carrier is $\cos(2\pi ft)$. The A_k and θ_k in the expansion for $V_n(t)$ above are the amplitude and phase, respectively, of the k -th harmonic of the fundamental and were controlled by an operator in order to achieve the best possible cancellation.

Figure 8 shows the configuration of the test setup used for this experiment. The upper channel provides a sinusoidally modulated 100 MHz carrier which is driven into a nonlinearity to create a third harmonic distortion product. The sinusoidal amplitude modulation for the 100 MHz fundamental is generated by a computer driving a D/A converter. This is described in more detail below. The third harmonic output of the nonlinearity is used as the input to the unweighted channel of the MX-500 ICS.

The lower channel provides the synthesized third harmonic by first generating a 300 MHz carrier through a bandpass limiter and then applying the synthesized third harmonic envelope by amplitude modulating the 300 MHz carrier. The harmonic modulation is derived from the computer as is the fundamental modulation. The resulting synthesized third harmonic amplitude modulated carrier is used as an input to the weighted channel of the MX-500 ICS. The ICS is used to effect the cancellation of the third harmonic interference from the nonlinearity by appropriately controlling the amplitude and phase of the synthesized third harmonic. The ICS output is monitored by use of a spectrum analyzer to measure the cancellation. The waveshape of the synthesized third harmonic amplitude modulation is varied by operator control to achieve the greatest cancellation at the ICS output.

In order to generate the fundamental and the synthesized amplitude modulation waveforms with the absolute phase coherence required and to permit the amplitude and phase of the harmonics in the synthesized modulation waveform to be independently controlled, these waveforms were digitally generated by a computer and D/A converter for use in the balanced modulators. The computer operated in two different modes in order to generate these waveforms: the compute mode and the output mode. In the compute mode the computer accepts commands from the operator via the CRT terminal. These commands established the values of A_k and θ_k for synthesis of the harmonic modulation waveform. After the operator entered A_k and θ_k for all $k = 0, 1, \dots, 7$ (this operation was simplified by entering changes only in order to expedite the optimization of the synthesized envelope), the computer generated two tables of data each 32 words long and stored them in memory. One table contained the values for the fundamental sinusoidal modulation ($\cos 2\pi ft$) while the second table

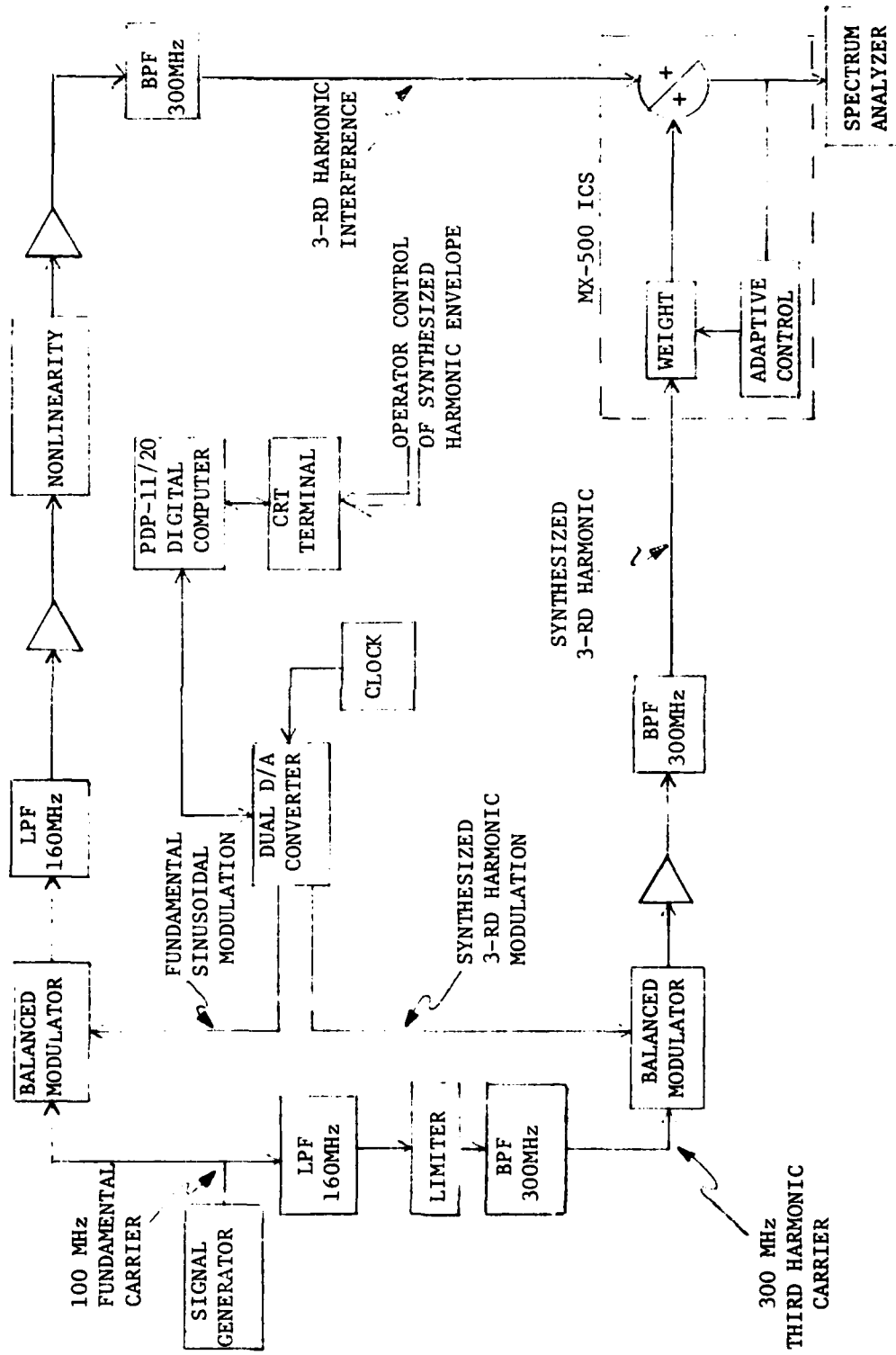


FIGURE 8. EXPERIMENTAL SETUP FOR FOURIER EXPANSION HARMONIC ENVELOPE SYNTHESIS

contained the values of the synthesized harmonic $V(t)$ as given in (3-1).

The second mode of operation commenced after the above tables were formed. In this mode the computer repetitively updated each of the two D/A converters with data from the appropriate table in memory, thus providing analog waveforms at the D/A converter outputs corresponding to the data stored in each table. The tables were read out repetitively by returning to the first entry after the last entry was used, thereby producing periodic waveforms. The fundamental frequency and hence the frequency of the first seven harmonics generated in this way was established by control of the frequency of the external clock supplied as an input to the D/A converters. In order to assure sufficient precision in the generation of the waveforms, system parameters and programs were established to provide at least four samples per period of the highest frequency used, the seventh harmonic of the fundamental modulation. The D/A converters were updated at a rate of $32f$, where f is the frequency of the fundamental modulation. With these parameters, the fundamental frequency could be as high as 940 Hz. The D/A converters have a resolution of 12 bits. Figure 9 is a photograph of the experimental setup.

The fundamental modulation frequency f has to be selected carefully within the following constraints. First, it must be a frequency low enough so that the D/A converter clock can run at $32f$. Second, it should be faster than the tracking speed of the MX-500 ICS so that the ICS does not follow the AM. Third, it should be low enough so that mismatches of the tunable UHF BPF's (approximately 500 kHz 3 dB bandwidths) do not limit the achievable cancellation. Fourth, f should exceed 300 Hz, so that the spectral lines are resolvable by a spectrum analyzer with a minimum resolution of 300 Hz.

The procedure for manually selecting the values of A_k and θ_k is based on the acquisition process that an adaptive system would follow if each harmonic were adaptively controlled by the LMS algorithm. The amplitude corresponding to the strongest sideband in the error signal at the ICS output is the one whose value should be changed most during the next LMS iteration. Hence, the manual adjustment procedure at each iteration is to vary the amplitude and phase corresponding to the strongest sideband in the error signal. This applies to all harmonics except the fundamental, which should be left at its maximum value since the MX-500 will adaptively adjust it. Therefore, the nulling procedure involves a trial and error approach of modifying the harmonic whose contribution to the ICS error output is greatest, continually seeking the set of $A_k, \theta_k, k = 0, 1, \dots, 7$ which provides the smallest residue.

Figure 10 shows the results of an experiment using the above procedure. The fundamental modulation frequency is 781 Hz. The upper photograph shows the spectrum of the ICS output with no cancellation (weighted channel disabled). The carrier frequency is 300 MHz and the sideband structure caused by the nonlinear third harmonic distortion is as shown. The lower photograph shows the cancelled ICS output after the adjustment procedure described above has been executed. The cancellation

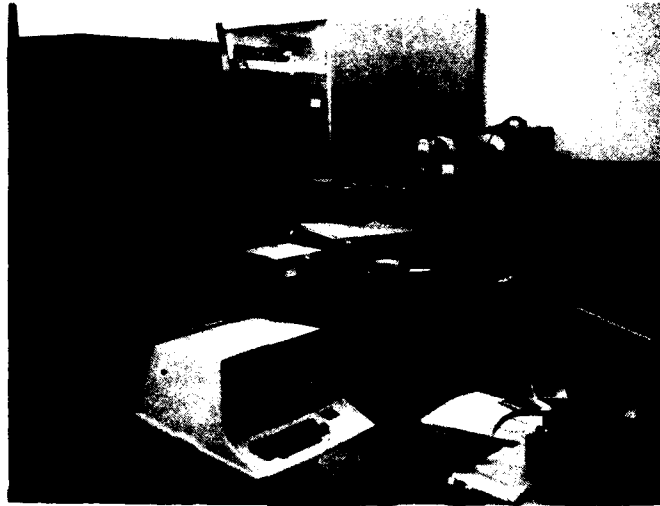
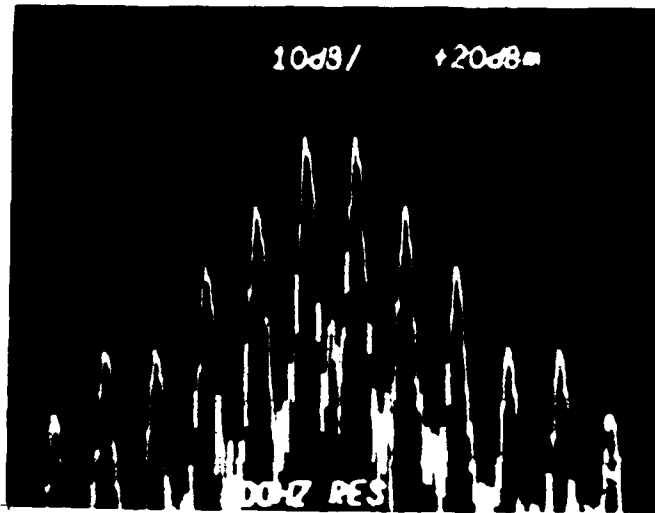
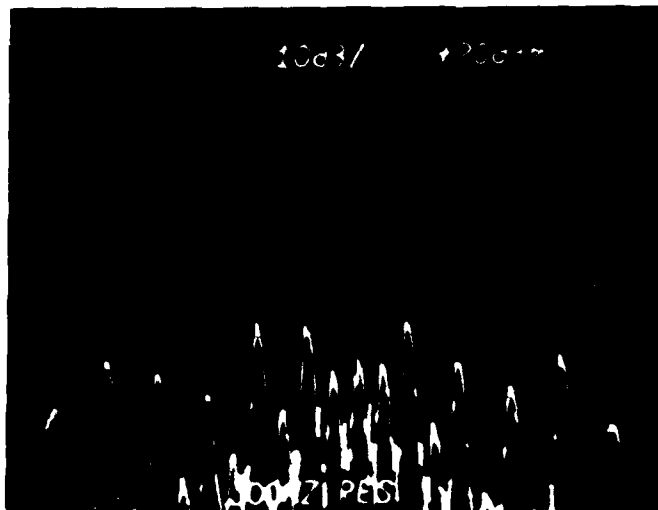


FIGURE 9
THE EXPERIMENTAL SETUP



UNCANCELLED ICS OUTPUT



CANCELLED ICS OUTPUT

CANCELLATION = 30 dB

FOR BOTH PHOTOGRAPHS:
 ANALYZER RESOLUTION=300 Hz
 VERTICAL: 10 dB/DIV
 HORIZONTAL: 2 kHz/DIV

FIGURE 10
 SPECTRUM OF THE ICS OUTPUT

for the central sidebands is 30 dB for the component at -900 Hz (with respect to band center), while the sideband at +900 Hz is cancelled by 35 dB. The sidebands at +2700 Hz, +4500 Hz and +6300 Hz are cancelled to a level below the residue at -900 Hz.

Note that sidebands at +8100 Hz and beyond are not cancelled at all since the synthesized harmonic envelope only includes terms up to the seventh harmonic (6300 Hz). Observe also that the spectrum of the cancelled residue is not symmetrical about the center frequency. This is due to AM-to-PM conversion effects in the test setup causing the two spectra at the ICS inputs to have slightly different sideband phases. The AM-to-PM conversion is caused by the fact that the test setup contains more than one nonlinearity. This effect is analyzed in Section 2.3.

Figure 11 shows the uncanceled and cancelled ICS output for the same experimental conditions as in Figure 10 except that the analyzer resolution is 3 kHz. This display provides a more integrated measure of ICS output and corresponds to what would be present in a 3 kHz wide receiver tuned to some part of the interference spectrum. The 30 dB cancellation at band center is clearly shown. Figure 12 shows the waveform of the synthesized harmonic modulation.

Table I is a tabulation of the amplitude and phases of the harmonic components of the synthesized harmonic modulation. The 0.001 amplitude value is the smallest amplitude that could be entered. Since this is more than 60 dB below the fundamental, these components have no effect on the results.

Table I - Harmonic Components of Synthesized Harmonic Modulation

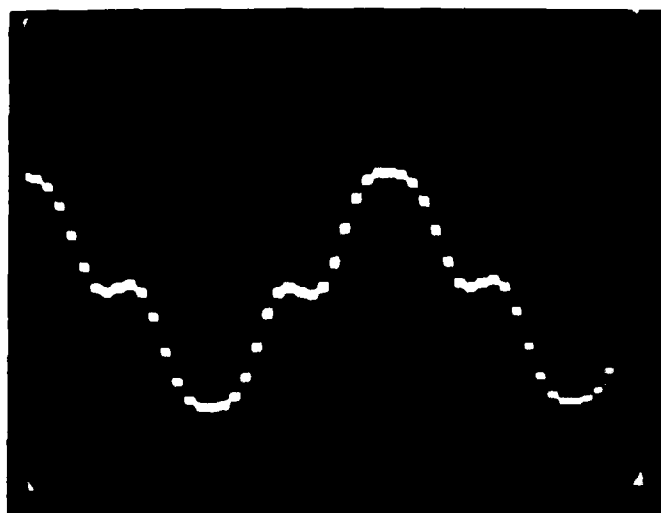
Harmonic Number (k)	Amplitude A_k	Phase θ_k ($^\circ$)
0	0.001	0
1	5.495	0
2	0.001	0
3	1.757	-4.5
4	0.001	0
5	0.446	180
6	0.001	0
7	0.1122	180



CANCELLED AND UNCANCELLED
ICS OUTPUT

ANALYZER RESOLUTION = 3 kHz
VERTICAL: 10 dB/DIV
HORIZONTAL: 2 kHz/DIV

FIGURE 11
ICS OUTPUT SPECTRUM



OSCILLOSCOPE TRACE

VERTICAL: 200 μ s/DIV

FIGURE 12
WAVEFORM OF SYNTHESIZED HARMONIC MODULATION

4.0 DISTORTION PRODUCT CANCELLATION SYSTEM CONFIGURATION

In this section the configuration of systems designed for the cancellation of harmonic and intermodulation distortion are described. These systems rely on some means of synthesizing the envelope of the distortion products (DP) involved from a knowledge of the fundamental envelopes. Two basic techniques for this synthesis are described. We begin by considering the cancellation of harmonic interference and apply the same concepts to the more general problem of intermodulation products (IMP).

4.1 HARMONIC ENVELOPE SYNTHESIS

Typically, the harmonic interference coupled into a receiver is due to only one of the harmonics of the offending transmitter. In this case the interference is given by (2-8) for an appropriate selection of harmonic number n . The objective of a harmonic interference cancellation system is to cancel the interfering harmonic signal to an acceptably low level by making use of the transmitted fundamental signal. Figure 13 shows the configuration of a system which cancels harmonic interference. The system operates by modulating a harmonic carrier with a synthesized harmonic envelope. The resulting synthesized harmonic is applied to the weighted channel of a standard ICS to provide cancellation. The ICS provides the amplitude and phase control of the synthesized harmonic RF (or IF) signal at a rate which is rapid enough to accommodate any changes in the coupling path from the nonlinearity to the receive antennas.

The harmonic envelope synthesizer operates on the envelope of the fundamental signal to create the envelope of the received harmonic. It is directed by the error signal from the ICS. The adaption time of the synthesizer is slow. Once adapted, it need respond only to changes in the characteristics of the nonlinearity which is assumed to be basically nonvarying.

The system of Figure 13 is adequate to cancel the harmonic distortion produced by one nonlinearity but will be unable to provide cancellation for the same harmonic produced by multiple nonlinearities (which need not be the same) excited by the same fundamental signal. As shown in Section 2.3, harmonic energy receive from multiple, memoryless nonlinearities exhibits phase modulation which is dependent on the amplitude modulation of the fundamental. This AM-to-PM conversion requires a more complex system to effect cancellation of the harmonic.

Figure 14 shows the configuration of a system for multiple nonlinearity generated harmonic interference cancellation. As can be seen, this system contains a synthesizer for both the inphase and quadrature components of the received interference. The inphase and quadrature components of the ICS output are used as feedback to the appropriate synthesizer. This system synthesizes an inphase and quadrature harmonic envelope and combines them exactly as Equation (2-18) indicates, thus matching the structure of the received interference.

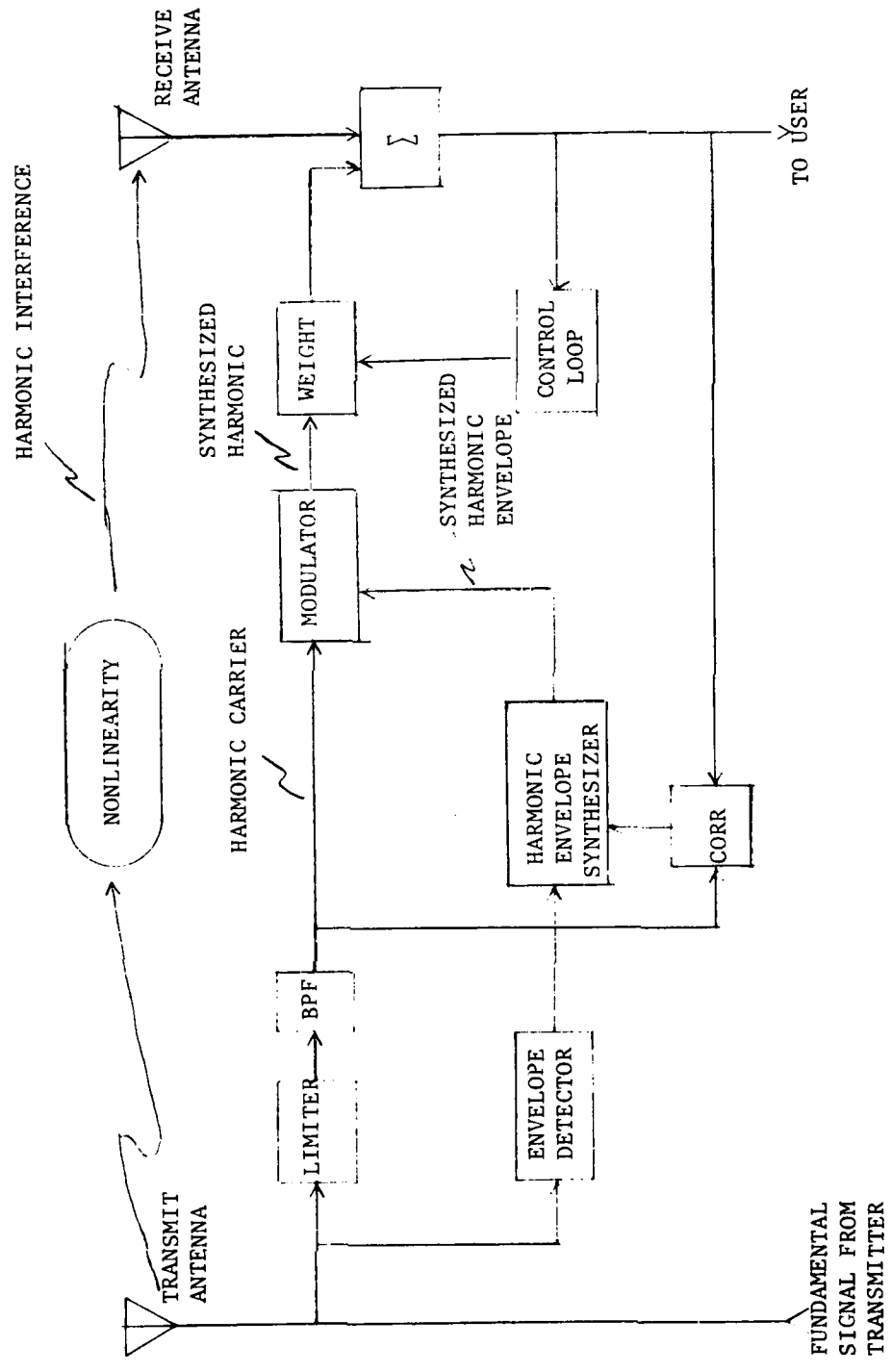
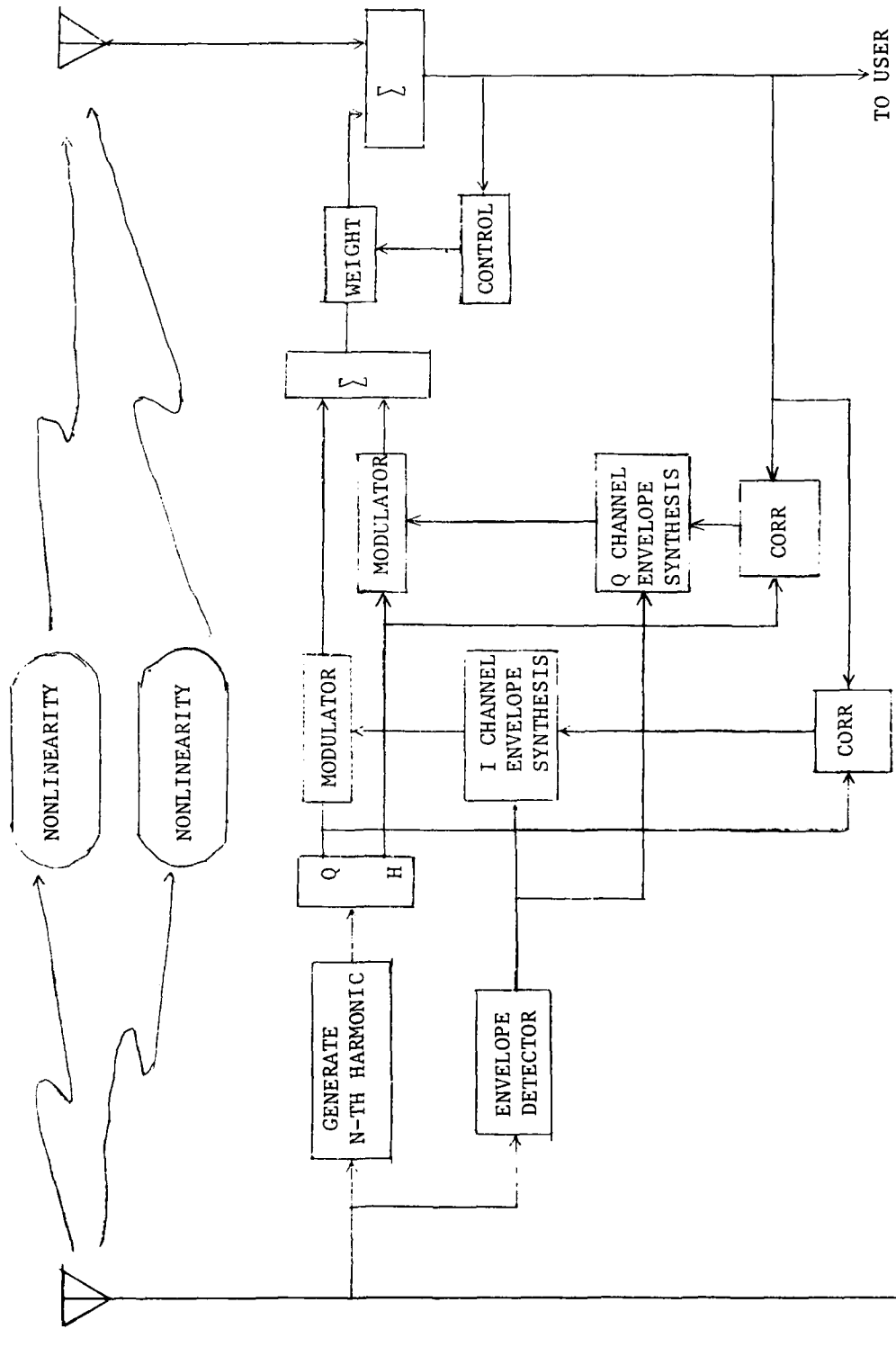


FIGURE 13. HARMONIC INTERFERENCE CANCELLATION SYSTEM



QH = QUADRATURE HYBRID
 CORR = CORRELATOR

FIGURE 14. HARMONIC CANCELLATION FOR MULTIPLE NONLINEARITIES

FROM
 FUNDAMENTAL
 TRANSMITTER

The crux of both systems described above is the synthesis of an harmonic envelope from knowledge of the fundamental. The residue from the ICS is available as feedback to guide the synthesis procedure. Means of implementing this synthesis operation are described in the following.

In the discussion which follows, $x(t)$ is used to denote the fundamental envelope. The first step in the synthesis of the envelope is the expansion of the fundamental envelope $x(t)$ in a convenient set of basis functions $g_i(x)$. The selection of the $g_i(x)$ is discussed later. A weighted sum of these basis functions is used to synthesize the envelope of the harmonic which we denote by $y(t)$. Thus the harmonic envelope is given by

$$y(t) = y[x(t)] = \sum_i c_i g_i[x(t)] \quad (4-1)$$

where the c_i are constants and the specific dependence of $y(t)$ on $x(t)$ is expressed by the first equality. Note that for the system shown in Figure 14, two synthesized envelopes $y_I(t)$ and $y_Q(t)$ are needed. The value of the c_i in the expansion for $y(t)$ above must be such as to minimize the power out of the ICS.

Figure 15 shows the operations required to implement the above processing. The fundamental envelope is expanded in the set of basis functions, $g_i(x)$ and each of these expansion functions is then multiplied by a constant c_i and summed. The figure shows the processing required for envelope synthesis in a cancellation system which has a single channel as shown in Figure 13. The summation of the weighted basis functions which is the synthesized envelope is used to modulate the harmonic carrier.

Adaptive control of the c_i is implemented by an LMS feedback loop which acts to minimize the output of the canceller. The LMS control loop is well suited to this application since it acts to minimize the output power of the canceller. The ICS output is first correlated (synchronously detected) with the synthesized carrier to extract the error at baseband and then is correlated with $g_i(x)$ to determine the error component associated with $g_i(x)$. This error signal is applied to the c_i multiplier through a lowpass filter.

The means of implementing the various signal processing operations shown on Figure 15 depends on the specific form selected for the $g_i(x)$. Several techniques of adaptively synthesizing the harmonic envelope have been identified. The approaches to envelope synthesis fall in two categories: gate functions and polynomial expansions.

4.1.1 Gate Function Synthesis

The use of gate functions in envelope synthesis is a straightforward approach well suited to digital processing circuits. Gate functions are binary valued functions which are useful for defining when a variable is within certain bounds. Formally, a gate function $g_i(x)$ is

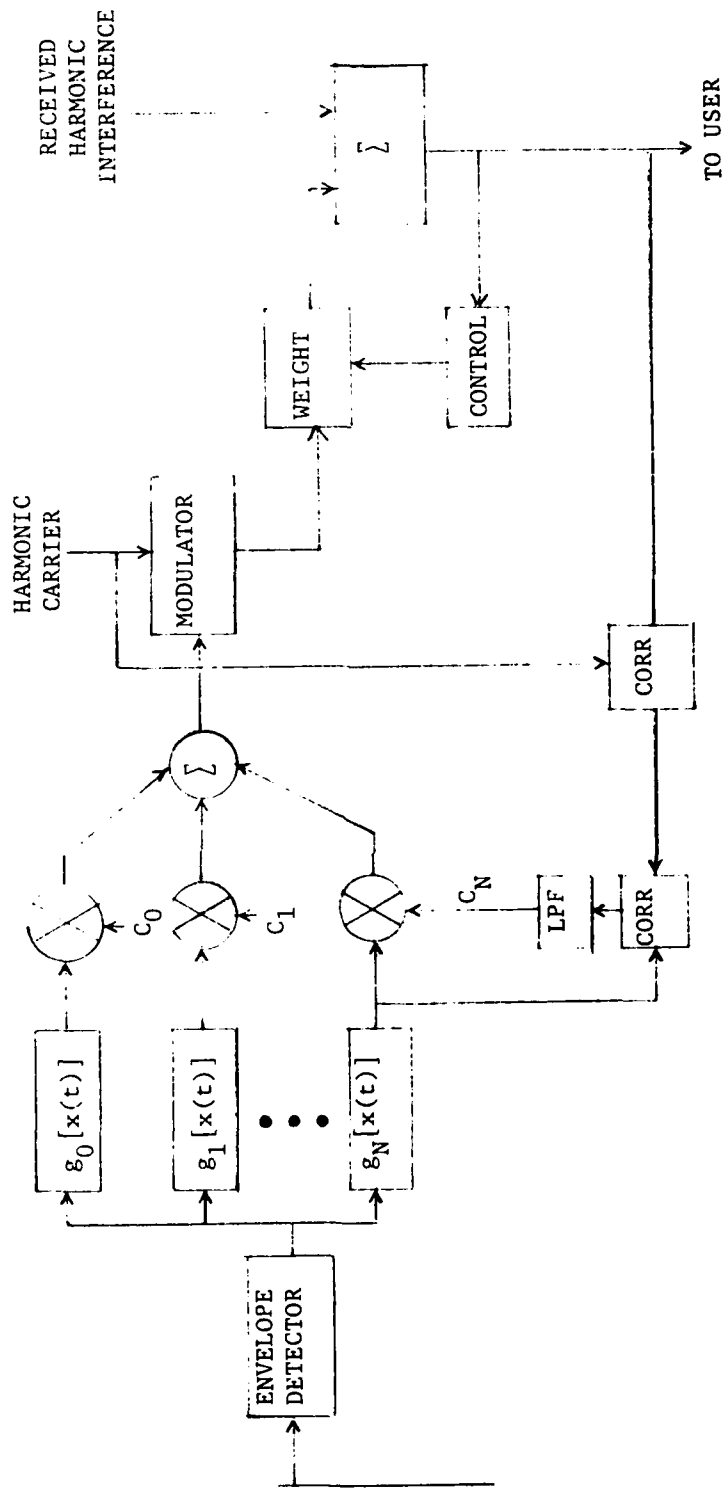


FIGURE 15. HARMONIC SYNTHESIS

defined as follows:

$$\begin{aligned} g_i(x) &= 1, \text{ if } x_{i-1} < x \leq x_i \\ &= 0, \text{ otherwise} \end{aligned} \quad (4-2)$$

for $i = 1, 2, \dots$. Figure 16 shows several gate functions. They can be used to expand an arbitrary function $f(x)$ as follows:

$$f(x) = \sum_{k=1}^N c_k g_k(x) \quad (4-3)$$

which is a stepwise function of x which can assume an arbitrary shape depending on the selection of c_k . For any x in an allowed range, one and only one g_k has nonzero value and $f(x)$ assumes the value c_k for that x . For our application, x represents the fundamental envelope and $f(x)$ represents the harmonic envelope. A typical $f(x)$ is shown in Figure 17. The objective of adaptive harmonic envelope synthesis is to select the set of c_k so that the system output is minimized.

A method is given in [11] for computing each c_n coefficient to minimize mean-square error $\overline{\epsilon^2}$ between the approximated output and a desired output $z(t)$. The value of c_n should be set so that $\partial \overline{\epsilon^2} / \partial c_n = 0$. This is achieved when the error

$$\epsilon = z(t) - \sum_{n=1}^N c_n g_n(x) \quad (4-4)$$

is orthogonal to each gate function, $g_n(x)$. Thus,

$$\begin{aligned} \overline{\epsilon g_n(x)} &= \overline{[z(t) - c_n g_n(x)] g_n(x)} \\ &= \overline{[z(t) - c_n] g_n(x)} \\ &= 0 \end{aligned} \quad (4-5)$$

where the overbar represents the averaging process used in defining the mean square error. If a time average is used, then adjustment of the coefficients $\{c_n\}$ to satisfy (4-5) in steady state may be implemented by the LMS (Least Mean Squares) feedback algorithm. Each coefficient is adjusted by a high gain negative feedback loop, which, in the steady state, satisfies Equation (4-5). The LMS algorithm generates an incremental negative feedback correction to each c_n that is proportional to the

[11] M. Schetzen, "Determination of Optimum Nonlinear Systems for Generalized Error Criteria Based on the Use of Gate Functions," IEEE Trans on Information Theory, January 1965, pp. 117-125.

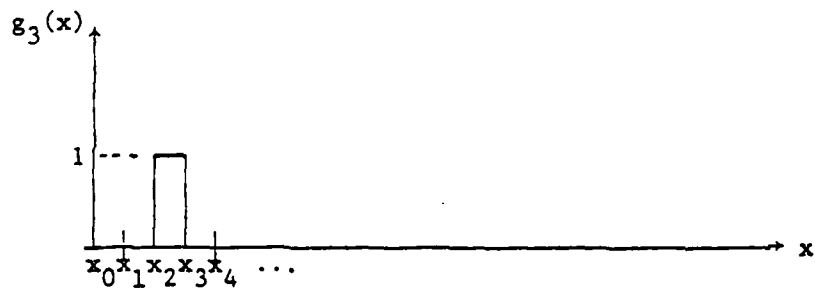
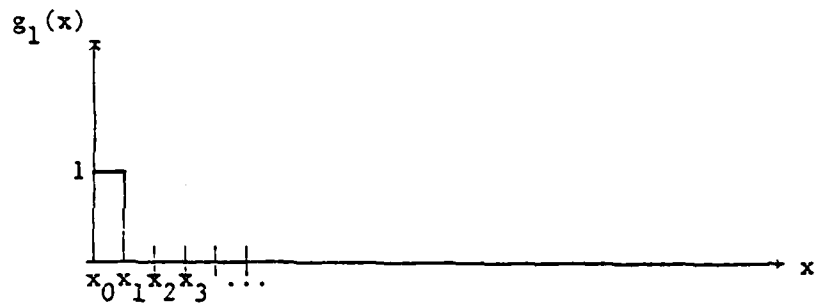


FIGURE 16
GATE FUNCTIONS

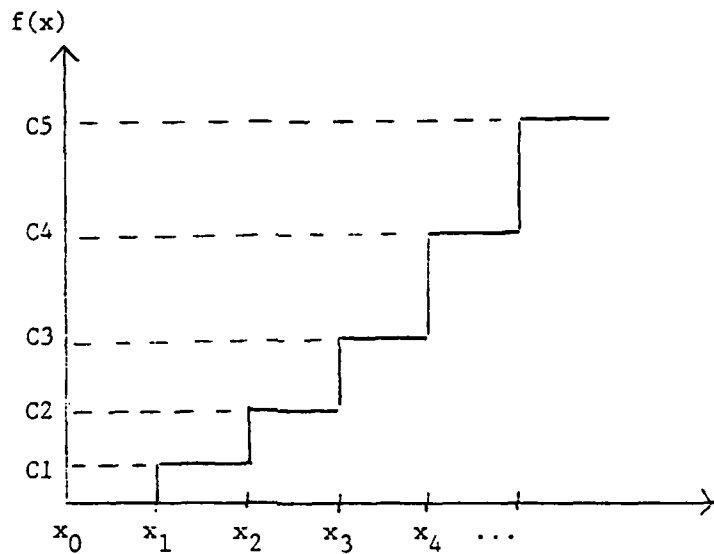


FIGURE 17
TYPICAL GATE FUNCTION EXPANSION

derivative of ϵ^2 with respect to c_n , that is:

$$\frac{dc_n(t)}{dt} = -\mu \frac{\partial \epsilon^2}{\partial c_n} = -2\mu \epsilon g_n(x) \quad (4-6)$$

Thus, in a sampled-date control system

$$c_n(j+1) = c_n(j) - 2\mu \epsilon(j) g_n[x(j)], \quad (4-7)$$

while in a continuous system

$$c_n(t) = -2\mu \int_0^t \epsilon(\tau) g_n[x(\tau)] dt \quad (4-8)$$

Equation (4-7) is particularly easy to implement digitally. It tells us that whenever the n -th gating function is activated, then c_n is incremented by $-2\mu\epsilon$ from its previous value. When the n -th gating function is not actuated, then c_n remains at its previous value. Since the gating function boundaries (x_n, x_{n+1}) do not overlap, only one gating function is activated at any one time. Thus, the weighted sum of gating functions used in (4-4) to approximate $z(t)$ reduces to

$$z(t) \approx c_n \quad \text{when } x_n < x(t) \leq x_{n+1} \quad \text{and } \epsilon \rightarrow 0 \quad (4-9)$$

If we apply $x(t)$ to an analog-to-digital converter that generates the number n when $x_n < x(t) < x_{n+1}$, then that number may be used to address a memory in which the c_n 's are stored. The addressed c_n is used to approximate $z(t)$ and is also updated to a new value by incrementing it by $-2\mu\epsilon$.

Figure 18 depicts the processing required to implement harmonic envelope synthesis using gate functions. The analog-to-digital (A/D) converted fundamental envelope is used as an address for the random access memory. This selection of a unique address for each unique code out of the A/D converter (corresponding to a range of envelope values) implements the gate function expansion described above. The number stored in the address represents the value c_k assigned to $g_k(x)$. The contents of the current address, c_k , are read out of memory and digital-to-analog (D/A) converted to form the input to the modulator. Adaptive control of the value of c_k is achieved by determining the error in the system output (by correlation) and incrementing the contents of the current address by a negatively scaled version of this error. (This processing implements the operations of (4-7) above which indicates that when the c_k reach steady state the error is small.)

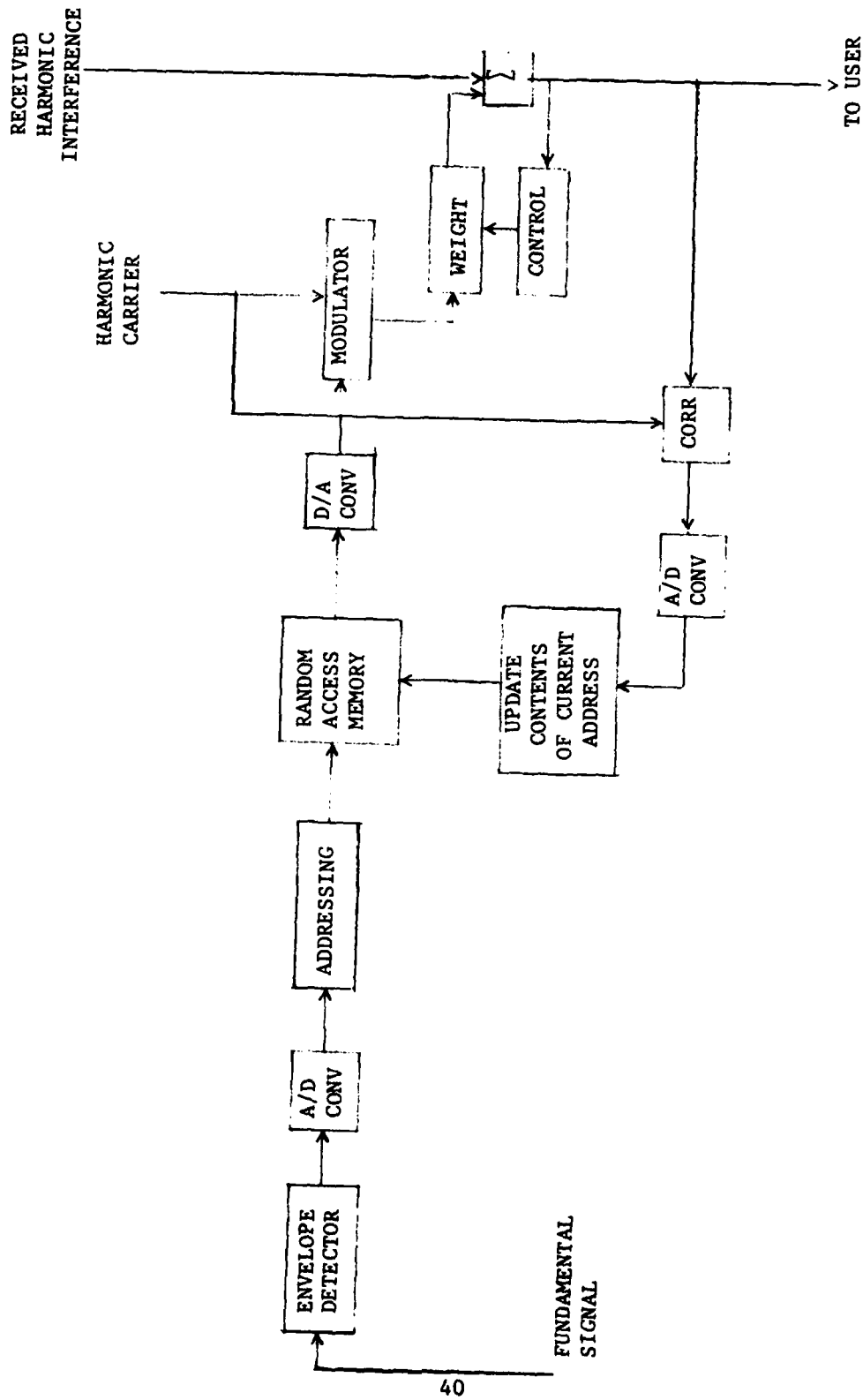


FIGURE 18. HARMONIC SYNTHESIS USING GATE FUNCTIONS

This implementation is seen to involve straightforward digital processing techniques where the only arithmetic operation involved is addition.

4.1.2 Polynomial Expansion Envelope Synthesis

An alternate means of expanding the nonlinearity to synthesize the harmonic envelope is to make use of standard polynomial expansions. A wide variety of possibilities is available. The simplest is a power series expansion in which the expansion functions are given by

$$g_i(x) = x^{i+n}, \quad i = 0, 1, \dots, N$$

where n is the order of the harmonic.

Other polynomials such as Tchebychev are available for expanding the nonlinearity. In this case the g_i are given by

$$g_i = x^n T_i(x)$$

where n is the order of the harmonic and $T_i(x)$ is the Tchebychev polynomial of order i . Several of these are listed below:

$$T_0(x) = 1$$

$$T_1(x) = x$$

$$T_2(x) = 2x^2 - 1$$

$$T_3(x) = 4x^3 - 3x$$

etc.

In either case the expansion of the harmonic envelope is given by:

$$f(x) = \sum_{i=0}^N c_i g_i(x) \quad (4-10)$$

where x is the fundamental envelope. As before, the coefficients c_i must be found to minimize the system output. Figure 19 shows the system configuration for utilization of polynomials in the synthesis of the harmonic. The envelope of the fundamental is A/D converted and the $g_i(x)$ computed for the envelope value x . Then $\sum c_i g_i(x)$ is formed and used to modulate the harmonic carrier. Adaptive control of each c_i is obtained by correlation with the harmonic carrier and then correlating each g_i with this error signal. Correlating each g_i with the error produces correction signals which are applied to the c_i to minimize the system output. The corrections are negatively scaled and lowpass filtered to implement the LMS control algorithm.

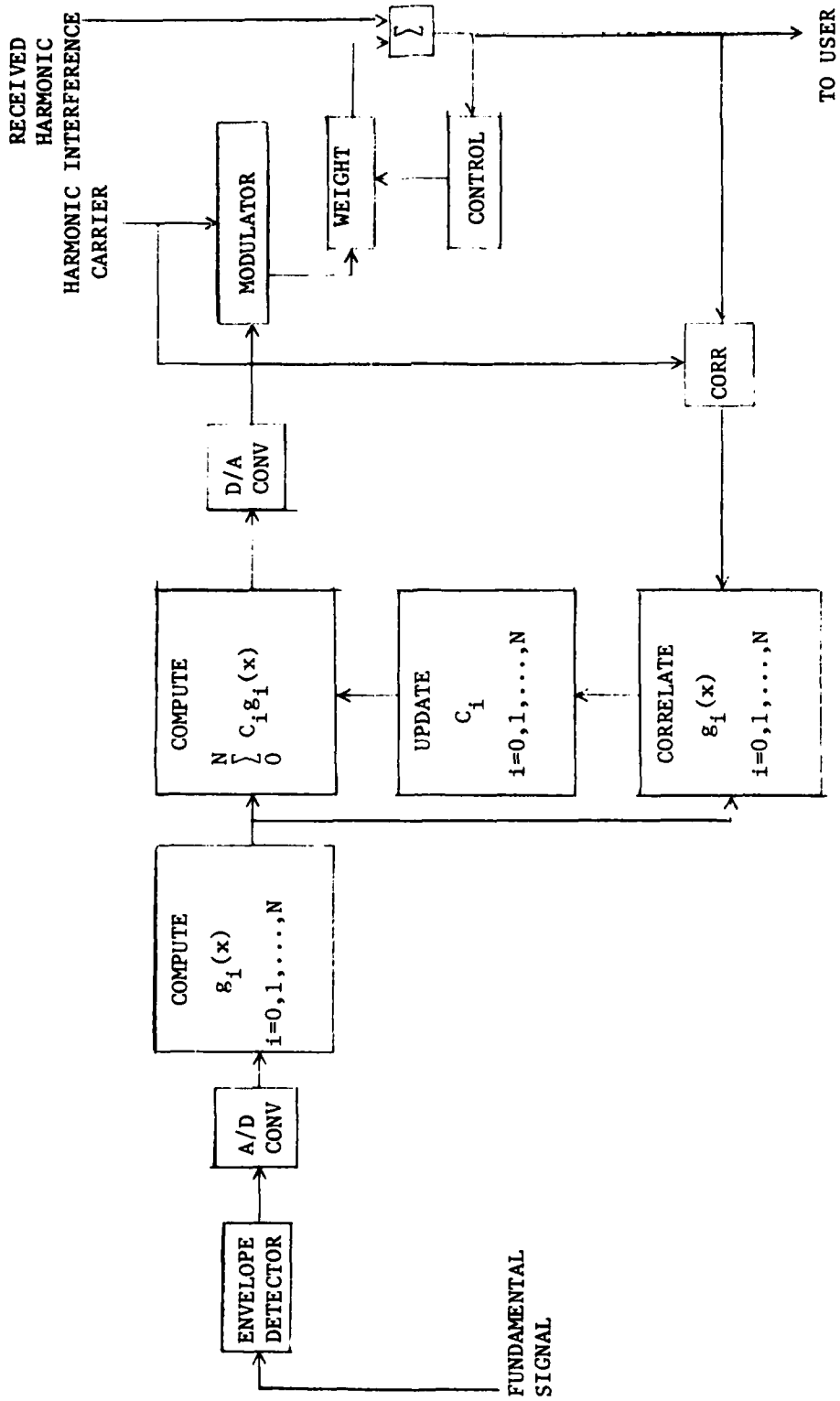


FIGURE 19. HARMONIC SYNTHESIS USING POLYNOMIALS

The response time of envelope synthesis can be improved by selecting expansion polynomials $g_i(x)$ that are orthogonal. Using orthogonal polynomials reduces the cross coupling in the correlation processing (ideally to zero) and permits the coefficients c_i to be found more rapidly. The Tchebychev polynomials are orthogonal and provide the additional advantage that minimization of the average power out of the canceller also minimizes the peak power.

As can be seen from Figure 19, considerably more arithmetic processing is required to synthesize the harmonic envelope using polynomial expansions in comparison to the gate function approach (refer to Figure 18). This processing is within the capabilities of today's digital processing components and can be done with a combination of table look-up and special purpose arithmetic processors.

4.2 INTERMODULATION PRODUCT SYNTHESIS

Intermodulation product (IMP) interference is produced when the fundamental signal from two distinct transmitters excite a nonlinearity and one of the resulting distortion components is coupled to the receive antenna of a receiving system. The objective of an IMP cancellation system is to cancel the interfering IMP to an acceptably low level by making use of only the fundamental signals. The structure of the IMP at a particular frequency $f_R = m_1 f_1 + m_2 f_2$ where f_1 and f_2 are the fundamental carrier frequencies is derived in Section 2.2. The IMP given by (2-15) where the amplitude modulation of the IMP $y(t)$ is expressed as a weighted summation of powers of the fundamental modulations.

Figure 20 shows the configuration of a system which operates to cancel IMP interference. The structure of this system is similar to that of the harmonic cancellation system. In the present case two fundamental signals must be processed to generate a carrier signal at the IMP frequency and to synthesize the IMP envelope. Generation of the IMP carrier can be accomplished by application of standard hardlimiting and filtering techniques. Synthesis of the IMP envelope, as before, is the difficult part of the system design.

Figure 21 shows the structure of the processing required for IMP envelope synthesis by a direct application of Equation (2-15) and its associated definitions (the equations following (2-15)). As these equations show the IMP envelope is a weighted sum of powers of the fundamental envelopes $A_1(t)$ and $A_2(t)$. The weighting coefficients c_{l_1, l_2} are related to the coefficients a_k of the power series expansion of the nonlinearity. These coefficients must be selected to closely approximate the received IMP envelope.

4.2.1 Synthesis of the IMP Envelope by Use of Gate Functions

The amplitude of the IMP at f_R can be synthesized using the gate functions described earlier in a system configured as shown in Figure 22. The system configuration is similar to that used for harmonic envelope

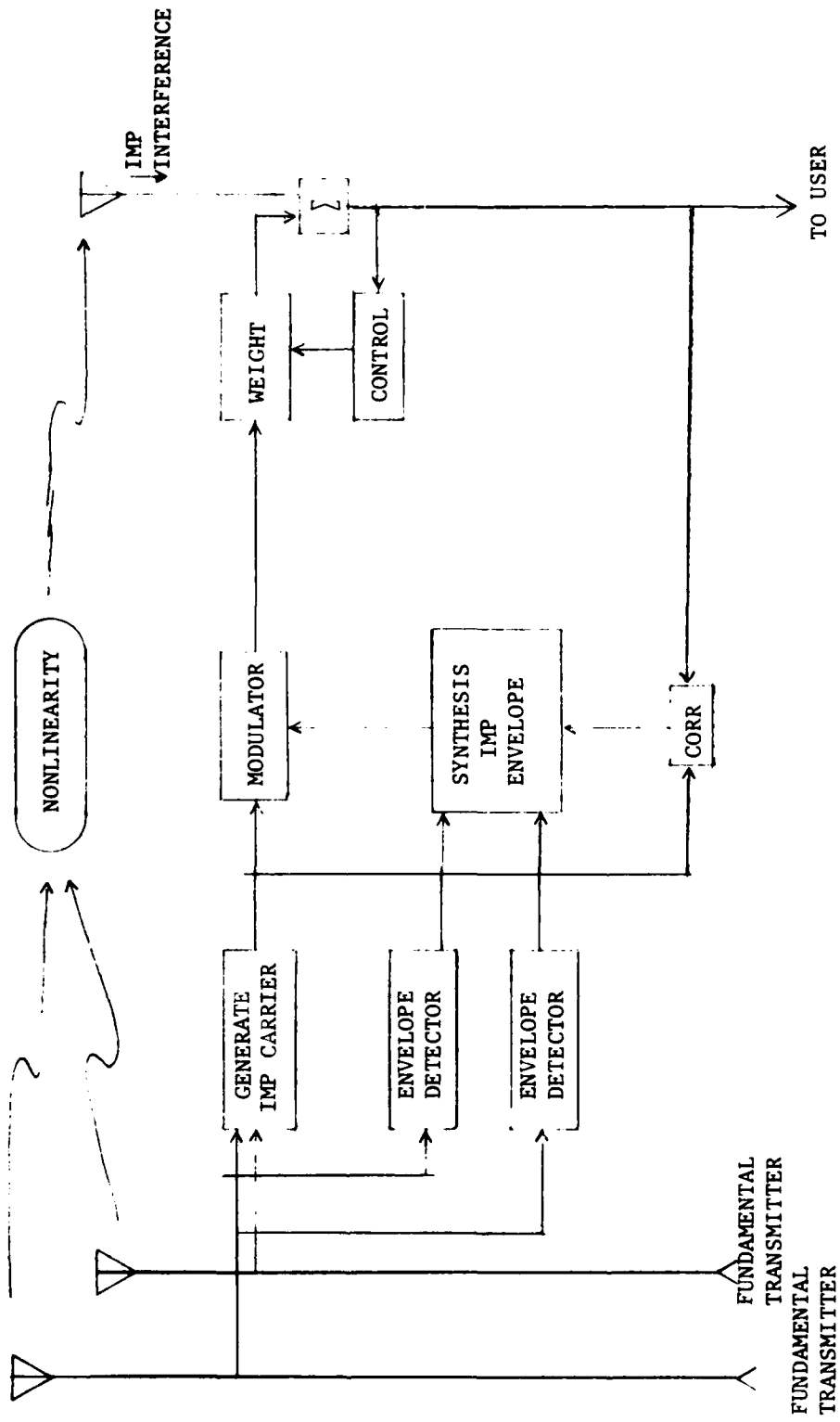


FIGURE 20. IMP CANCELLATION SYSTEM

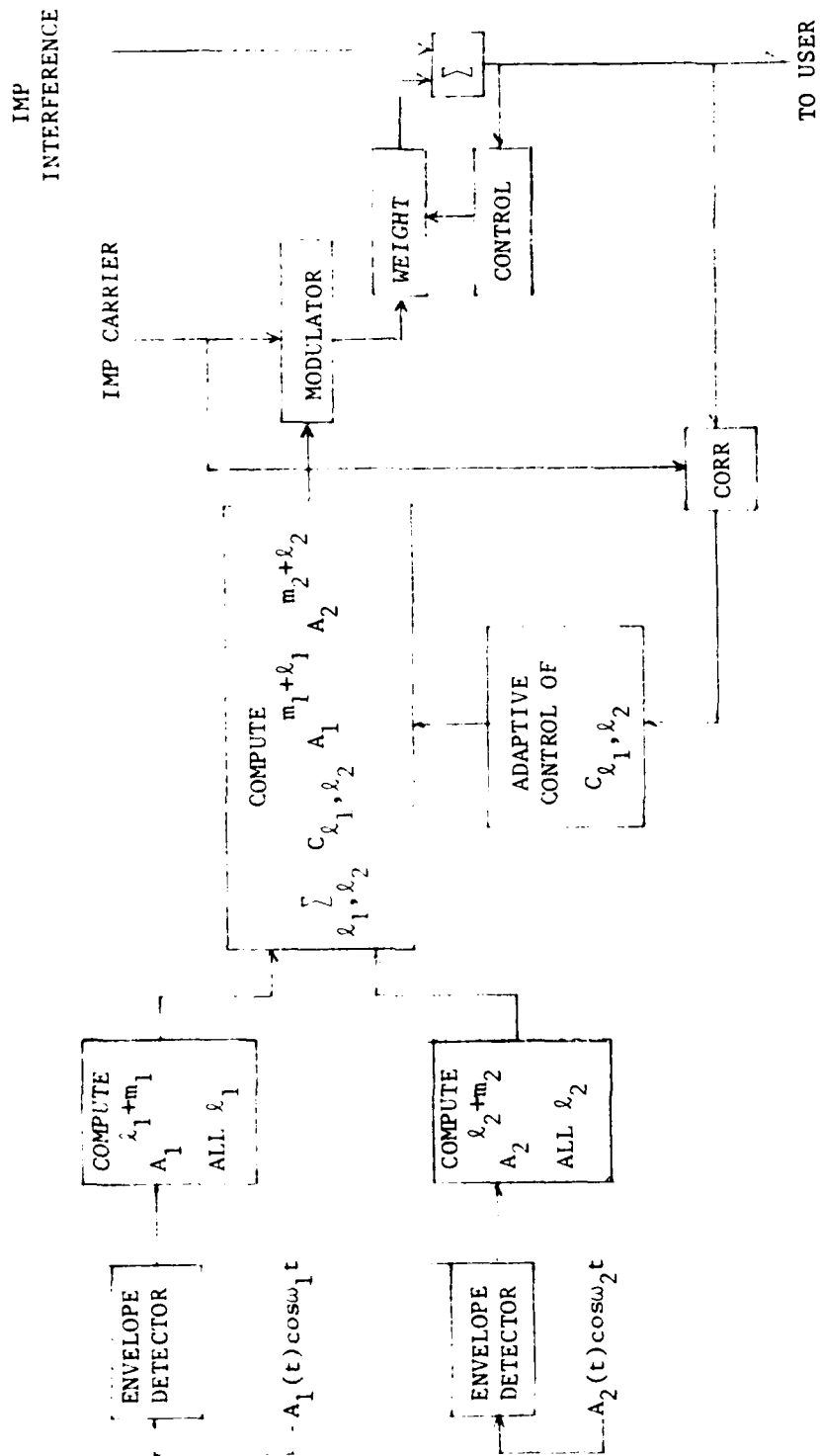


FIGURE 21. SYNTHESIS OF IMP AMPLITUDE MODULATION

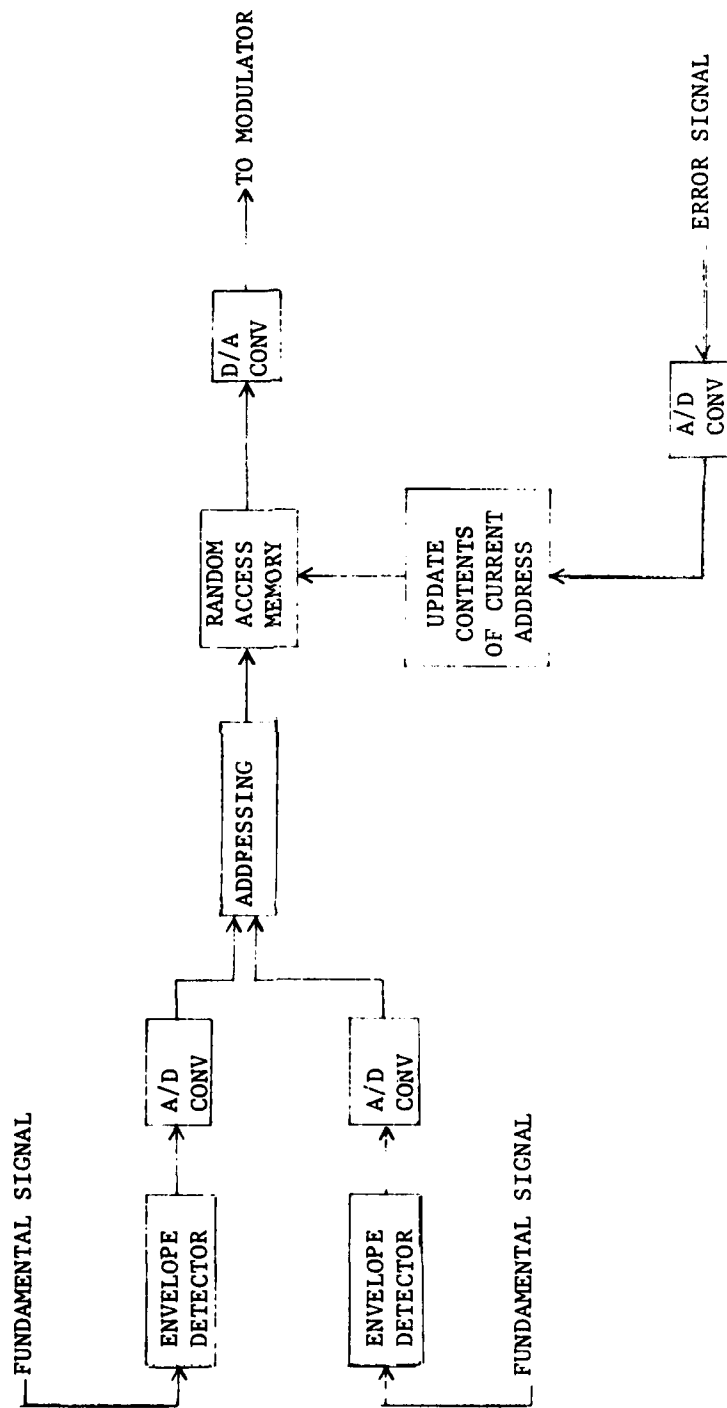


FIGURE 22. IMP ENVELOPE SYNTHESIS USING GATE FUNCTIONS

synthesis (refer to Figure 18). The output of each fundamental transmitter is A/D converted and used to address into a random access memory. When used for harmonic envelope synthesis, the output of a single A/D was used to address into a particular memory location, thus implementing the gate function processing. For the harmonic case, the memory was one-dimensional, that is, each A/D converter output selected one memory location. For use in the synthesis of IMP envelopes, the memory is two-dimensional, that is, the A/D output of one fundamental envelope determines the value of one coordinate and the A/D output of the second fundamental determines the value of the second coordinate. A particular memory location is determined by both A/D outputs, thus implementing a two-dimensional gate function.

The contents of the memory location addressed in this way contain a constant which is the amplitude of the IMP corresponding to the two fundamental envelopes. The value of this constant is continually updated by the operation of an LMS control loop as was done in the harmonic envelope case and defined by Equation (4-7).

Because of the need to drive the IMP synthesis processing from two fundamental envelopes, the size of the memory required will increase substantially. In addition, due to the increased number of memory locations, the time required for the synthesis processing to converge to its steady state will be greatly increased over the adaption time for the harmonic envelope synthesis case.

4.2.2 Polynomial Expansion IMP Envelope Synthesis

As was done in the case of harmonic envelope synthesis, polynomial expansion can be used to synthesize the IMP envelope. To see how this is done, we begin by expanding the fundamental envelope terms of the IMP $y(t)$ derived earlier (see Equation (2-15)) as follows:

$$A_1^{\ell_1} = \sum \beta_r(\ell_1) g_r(A_1)$$

$$A_2^{\ell_2} = \sum \beta_s(\ell_2) g_s(A_2)$$

where the coefficients $\beta_r(\ell_1)$ and $\beta_s(\ell_2)$ can be computed exactly once the form of $g_i(x)$ is selected. Using these representations in $y(t)$ as given in (2-15), the IMP envelope derived in Section 2.2, and interchanging orders of summation, $y(t)$ can be expressed as

$$y(t) = A_1^{m_1} A_2^{m_2} \sum_r \sum_s b_{r,s} g_r(A_1) g_s(A_2) \quad (4-11)$$

where

$$b_{r,s} = \sum_{l_1=r}^{L_1} \sum_{l_2=s}^{L_2} c_{l_1,l_2} \beta_r(l_1) \beta_s(l_2)$$

Figure 23 shows the system configuration which implements the above processing. Its structure is similar to that used for polynomial expansion of harmonic envelopes shown in Figure 19. As shown in Figure 23, control of the coefficients $b_{r,s}$ is implemented by use of an LMS control loop. The correlation and updating processing implements the control algorithm shown in Figure 14.

The arithmetic processing required to implement the operations shown in Figure 23 is much greater than for the gate function synthesis approach shown in Figure 22. However, the memory requirements are less and the acquisition time should be more rapid. More study is required to compare the performance and complexity of the two IMP envelope synthesis approaches.

4.2.3 System Configuration for Multiple Nonlinearities

As was the case for harmonics, multiple nonlinearities will produce AM-to-PM conversion effects for IMP. By providing separate synthesis capability for I and Q channels, it should be possible to generate a replica of the composite received IMP. More study is required to evaluate this approach and to investigate means of reducing its complexity. Such a system is roughly twice the complexity of the systems shown in Figure 22 or 23.

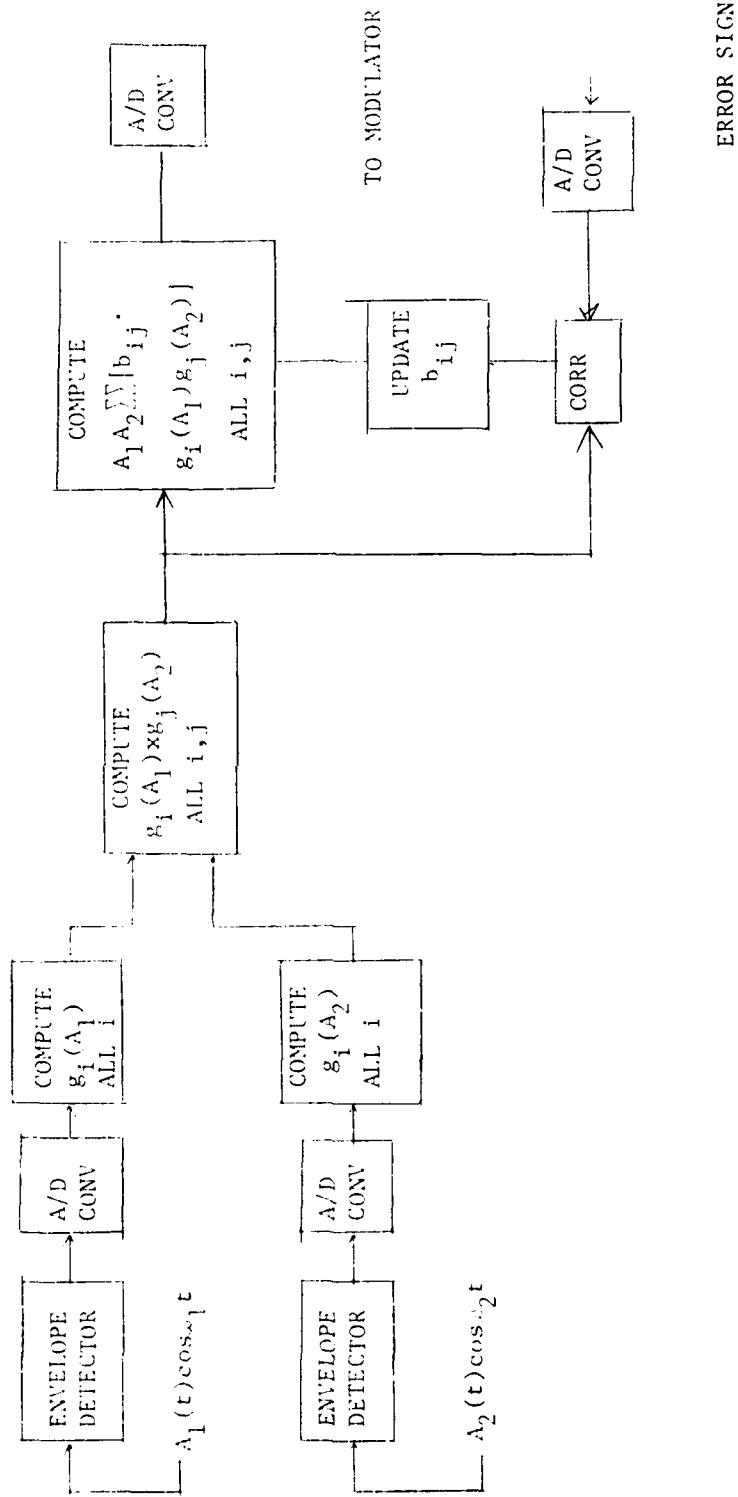


FIGURE 23. IMP ENVELOPE SYNTHESIS USING POLYNOMIALS

5.0 SIMULATION OF ENVELOPE SYNTHESIS BY GATE FUNCTIONS

In order to determine the effectiveness of an harmonic cancellation system which employs gate function synthesis of the harmonic envelope, system operation was simulated on a digital computer and the performance of the system evaluated for a variety of external nonlinearities and fundamental amplitude modulation waveforms. The simulation was configured in such a way as to accurately represent the digital processing that would be implemented in a practical system realization. In the following, the simulation is described in detail and the results discussed.

5.1 DESCRIPTION OF SIMULATION

The harmonic cancellation system simulated is that shown in Figure 14 which includes separate I and Q channels to properly synthesize the harmonic envelope for the situation where there is AM-to-PM conversion due to the presence of multiple nonlinearities. The I and Q channel harmonic envelope synthesis is implemented by use of gate functions as shown on Figure 18.

The simulation operates with the complex envelopes of all RF signals actually present in the system. Therefore, the ICS which produces the cancellation by weighting the synthesized harmonic and combining it with the received interference is not included in the simulation of the system. This exclusion is not significant in terms of the evaluation of the harmonic cancellation system performance, since the ICS performance is not the limiting factor in this system. Its functions to adjust the amplitude and phase of the synthesized harmonic in order to compensate for small differences in the interference coupling path.

Figure 24 shows the structure of the simulation. The simulation program was written in FORTRAN and run on a PDP-11/35 computer. Each iteration of the program begins with the generation of a sample of the fundamental modulation waveform. This sample is used to generate a sample of the output of at least one nonlinearity. Up to three nonlinearities were simulated at one time. All nonlinearities were modelled as polynomial functions of the fundamental waveform.

The fundamental sample is also used to generate the phase of the synthesized harmonic carrier. The carrier phase is the angle of the (possibly) complex-valued fundamental amplitude modulation waveform. In order to assure that carrier is present for both I and Q channels, a fixed 45° phase offset was added to the phase found as described above. The envelope detector function is accomplished by forming the magnitude of the fundamental. The function of A/D conversion is implemented, by converting from floating point to integer representation in the simulation program. Prior to integer conversion, the envelope is clipped to represent the effect of an A/D converter with a limited number of bits.

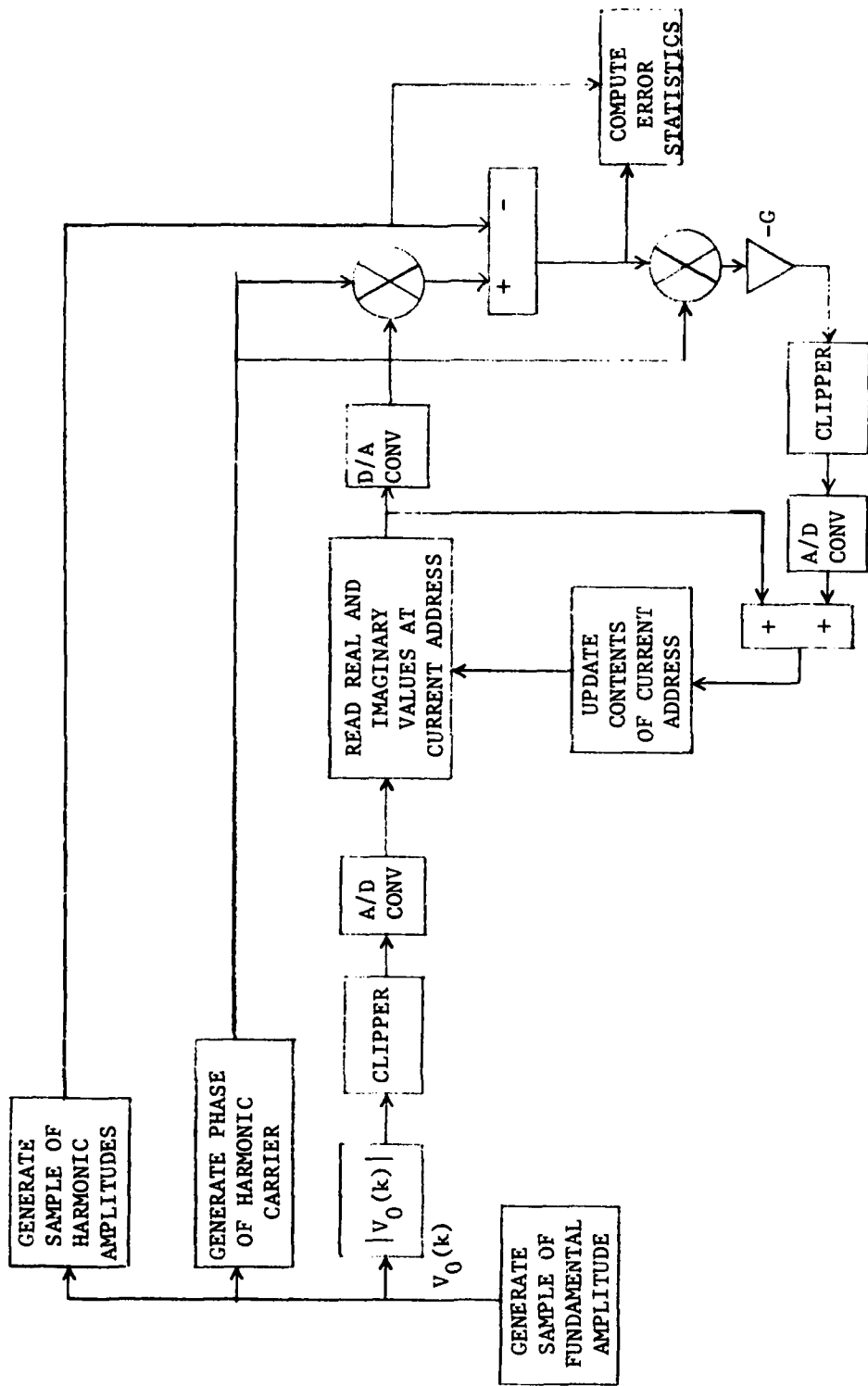


FIGURE 24. HARMONIC ENVELOPE SYNTHESIS SIMULATION

The clipper function is the following, where Y is the clipper output.

$$Y = |v_0| \quad \text{if } |v_0| \leq 2^N - 1$$
$$= 2^N - 1 \quad \text{if } |v_0| > 2^N - 1$$

This clipping function, when followed by integer conversion, represents the operation of an A/D converter with N-bit output resolution.

The integer output of the A/D converter is used as an address to select one entry from each of two tables. The two tables represent the I and Q components of the synthesized harmonic envelope and the addressing described above implements the mathematical structure of the gating function. The bit length of each entry in the tables was restricted to N bits to accurately represent a practical system implemented with fixed point arithmetic and N-bit processing and storage capabilities.

The addressed I and Q table values are D/A converted to floating point representation and multiplied by the complex the complex envelope of the synthesized harmonic carrier (unity magnitude) to form the synthesized modulated harmonic. The complex-valued harmonic interference is subtracted from the synthesized harmonic to form the canceller error signal. After multiplication by the synthesized harmonic carrier to effect correlation or synchronous detection and negative amplification, the error is clipped and A/D-converted to an N-bit integer number as described earlier. The current I and Q values are added to the resulting error signal and the results loaded into the tables as the new I and Q values. The new I and Q values are clipped at a level of $2^N - 1$ to represent storage limitations of N-bit words.

The processing described above implements the LMS control algorithm for both the I and Q values of the synthesized harmonic envelope. When a particular entry in the I and Q tables is addressed, the updating equation for those values is

$$X(k+1) = X(k) - G\varepsilon$$

where $X(k+1)$ = new value

$X(k)$ = old value

ε = error at the canceller output

G = gain in error path

The above disregards the operation of the clipper and A/D converter.

The simulation program included the definition of the fundamental waveform and the number and form of the nonlinearities. At run time the following parameters could be selected:

Number of bits (N)
Sample rate
Gain (G)
Fundamental waveform frequency
Run time

The output data from the program is the time history of cancellation defined as

$$C = 10 \log(\overline{|\epsilon|^2} / \overline{|v_n|^2})$$

where $\overline{|\epsilon|^2}$ = average of the squared error at canceller output

$\overline{|v_n|^2}$ = average of the squared harmonic interference

The value of $\overline{|v_n|^2}$ is also provided as an output. The average is computed over one hundred samples of the respective signals.

An additional output is available on an optional basis. A plot of the values of the I and Q synthesized harmonic tables can be obtained.

Generally, the maximum levels of both the fundamental waveform and the harmonic interference are set to utilize nearly the full dynamic range provided by the number of bits N. That is, the maximum values were selected to be approximately 0.9 or 0.95 times 2^N .

Details of the simulation are available from the FORTRAN program listing in Appendix B.

5.2 SIMULATION RESULTS

The simulation program was run for a variety of fundamental waveforms, nonlinearities, numbers of nonlinearities and canceller system parameters. The results of these various runs indicate that the gate function synthesis approach is capable of creating the harmonic envelope by making use of knowledge of the fundamental amplitude modulation.

A variety of fundamental amplitude modulations were used. The following are typical examples.

Amplitude modulation (AM): $A(1 + a \sin \omega t)$, $a < 1$

AM/Suppressed carrier (SC): $A \sin \omega t$

Multi-tone (MT) AM/SC: $A_1 \sin \omega_1 t + A_2 \sin \omega_2 t$

Generally the fundamental modulation was selected to have a maximum amplitude less than unity. The result was then scaled prior to entry into the envelope detector. The scaling constant is 2^{N-1} , the dynamic range of the A/D converter for any value of N.

The same scaling is applied to the output of the composite nonlinearity with the nonlinearity characteristic selected to yield a maximum envelope of less than unity. This scaling assures that the full dynamic range of the N-bit words in the I and Q envelope synthesis tables is utilized without overflow. The following nonlinearities were used in various combinations for simulation runs.

A. Diode Approximation

$$v_3 = \frac{v^3}{6} \left(1 + \frac{v^2}{4} \left(1 + \frac{v^2}{10} \left(1 + \frac{v^2}{18} \right) \right) \right)$$

where v = fundamental amplitude

v_3 = third harmonic amplitude

This approximation is from reference [6].

B. Third-Order Polynomial: $v_3 = A_1 v + A_3 v^3$

C. Fifth Power of Fundamental: $v_3 = A v^5$

These nonlinearities represent distributed nonlinearities as described in Section 2.3. Therefore, the harmonic amplitudes of each separate nonlinearity are combined with different RF phases to produce a complex, composite harmonic interference at the input to the canceller. All simulations were formally run for the third harmonic case although the results are general and apply to higher order harmonics.

Table II contains a summary of the results of typical simulation runs for a variety of simulation parameters. The fundamental modulation and nonlinearities have been defined above.

Multiple entries in the nonlinearity column indicate that those nonlinearities were present simultaneously to produce a composite nonlinearity. The column entitled "Special Conditions" indicates the deviations from the standard conditions made during certain of the simulation runs. Average harmonic power is the mean square value of the harmonic interference at the canceller input with a 0 dB reference of 1 watt. Average steady state (SS) cancellation is given by

$$C = 10 \log \left(\frac{|\epsilon|^2}{|V|^2} \right)$$

where $|V|^2$ = mean square harmonic interference

$|\epsilon|^2$ = mean square canceller output

The final column, the acquisition time, is a measure of the time taken for the cancellation to reach a level within 2 to 4 dB of the steady state cancellation. The values listed in this column are not precise and should be taken as an approximate measure of the time for the harmonic envelope synthesis to settle.

TABLE II
SUMMARY OF SIMULATION RESULTS

<u>Entry</u>	<u>Fundamental</u>	<u>Nonlinearity</u>	<u>Special Conditions</u>	<u>Av. Harmonic Power (dB)</u>	<u>Av. SS Cancel'n (dB)</u>	<u>Acquisition Time (sec)</u>
1	AM/SC, AM	A, B, C	-	56	56	2.0
2	AM/SC	A, B, C	-	46	49	2.0
3	AM/SC	A, C	-	62	62	2.0
4	AM/SC	A, C	N=9	52	52	0.2
5	AM/SC	A, C	N=7	40	40	0.05
6	AM/SC	A, B	-	64	65	2.0
7	AM/SC	A, B	G=0.25	64	25	1.1
8	AM/SC	C	-	59	61	2.0
9	MT-AM/SC	B	-	60	62	1.2

Standard Conditions: Number of Bits, N = 11

Gain, G = 1.0

Sampling Rate = 10,000 samples/second

Study of simulation output data indicates that cancellation starts at 0 dB and improves, finally reaching the indicated steady state value. However, the improvement is not smooth and continuous. The cancellation is observed to increase steadily for a time period and then decrease for a short interval, returning to better cancellation after the sharp decrease.

The reason for this is the fact that a particular entry in the I and Q synthesis tables is updated only at those times when the fundamental envelope falls in the range of signal levels which yield the proper address. During the adaption process certain table entries are skipped over more than others and, therefore, remain in their initial zero or partially adapted state for a longer time. The time at which they begin to adapt or resume adaption occurs when the fundamental is sampled at the correct time to produce the required address. This process can lead to situations where the adaption of certain table entries takes considerably longer than other entries, thus producing bursts of poor cancellation during the adaption process.

Another factor affecting the cancellation data is the way in which they are computed. The mean square canceller output is found by arithmetically averaging the squared magnitude of the error signal over blocks of 100 samples. This averaging over blocks also tends to produce somewhat nonuniform results.

The acquisition time listed in Table II is the approximate time it takes for the cancellation to remain within 2-4 dB of the final value with no short intervals of poor cancellation.

As the data in Table II indicate, the harmonic envelope synthesis can be accomplished very accurately. For those cases where the gain is unity, the steady state cancellation is about equal to the average harmonic power. The limitation to ultimate cancellation in these cases is the limited number of I and Q table entries ($2^N - 1$ locations) and the limitation of each of these to N bits. These two effects appear as a minimum resolution, placing a lower bound on the achievable cancellation. Note, that the case where $G = 0.25$ (entry 7) achieves considerably reduced cancellation.

The acquisition time for those cases run under standard conditions is between 1 and 2 seconds. For entries 4 and 5, the acquisition time is greatly reduced from this, because there are many fewer I and Q synthesis table entries to update. The acquisition time for entry 7 where the gain is reduced is smaller than those cases run with standard conditions because the steady state cancellation is lower. The 1.2 second acquisition time for entry 9 which is for the multi-tone AM/SC case indicates that variations in fundamental envelope waveform affect the settling time of the synthesis procedure.

The values of the I and Q synthesis tables are plotted in Figure 25 for the simulation run of entry 6 in Table II. For this simulation run,

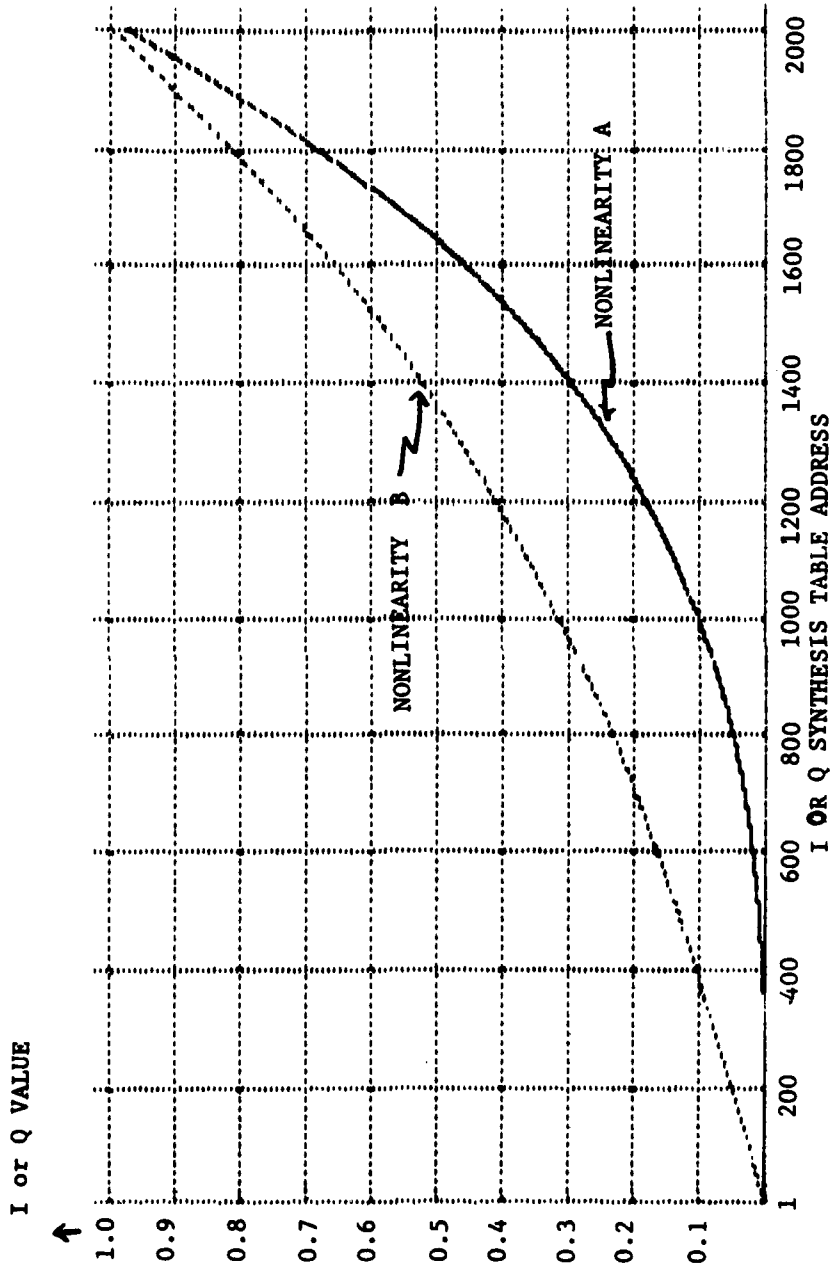


FIGURE 25
SYNTHESIZED I AND Q NONLINEARITIES

the RF phases of the A and B nonlinearities were selected to align exactly with the phases of the I and Q components of the synthesized harmonic carrier, respectively. The result of this alignment is that the I channel adapts to synthesize nonlinearity A while the Q channel adapts to synthesize the B nonlinearity. Figure 25 is a plot of the normalized value of A and B synthesis tables as a function of the address of the tables. The plot is normalized to the maximum value in either the I or Q table. Each curve represents the nonlinear transfer function of the appropriate nonlinearity.

6.0 CONCLUSIONS AND RECOMMENDATIONS

This study was directed at the analysis of the characteristics of harmonic interference and the synthesis and evaluation of techniques to effect cancellation of such interference. The results were extended to indicate approaches to cancellation of more complex distortion product (DP) interferences including harmonics from multiple nonlinearities and intermodulation products caused by two fundamental signals. During the initial stages of the investigation, a survey of the literature was conducted in order to determine if any existing work was available to assist in the problem formulation or solution. In spite of the current renewed interest in nonlinear system analysis, no work was uncovered which addressed the problem from the standpoint of detailed harmonic or DP waveform analysis; hence the available work is not directly applicable to the DP cancellation problem.

In addition to the analysis of harmonic waveforms, extensive laboratory experiments were conducted to evaluate the extent to which typical nonlinearities are memoryless. The conclusion of these experiments is that, at least to a level corresponding to 20 to 30 dB of cancellation over limited bands, the nonlinearities are memoryless. These experiments also provided initial verification of the concept of harmonic envelope synthesis for harmonic interference cancellation.

Further evaluation of harmonic envelope synthesis by use of gate function processing was obtained by simulating the essential parts of a harmonic cancellation system. The results of the simulation indicate that the approach is viable and realizable with available analog and digital signal processing components. The complexity of such an implementation appears to be reasonable.

The results of the study indicate that a harmonic cancellation system employing the concept of harmonic envelope synthesis is feasible and that the next step should be the design and implementation of an experimental canceller. Many practical design issues remain to be resolved prior to implementation. Among them are the following.

The effect of variations in the coupling between the fundamental transmitter and the harmonic producing nonlinearities. Such variations may require more rapid synthesis adaptation or greater dynamic range.

Coupling variations between the nonlinearity output and the victim receiver may be completely accommodated by the ICS or may need additional level control processing.

The effect and relationships between various fundamental waveforms and the synthesis update rate.

A consideration of the total RF bandwidth that must be processed at the victim receiver input to properly represent

the received harmonic envelope.

Optimization of the number of bits and the memory size requirements for a desired level of cancellation. This should include a consideration of nonlinear A/D and D/A conversion characteristics (companding) to make most effective use of the available dynamic range.

With these system-related questions resolved, the design of an experimental model can proceed. Of course, many design issues remain to be resolved, but these are the typical implementation questions associated with any canceller system design.

APPENDIX A

CANCELLATION ACHIEVABLE BY DIFFERENT NONLINEARITIES

A1.0 INTRODUCTION

As derived in Section 2, the waveform at the output of a nonlinearity characterized by the power series expansion

$$v_{OUT}(t) = \sum_{k=0}^{\infty} \alpha_k v_{IN}^k(t) \quad (A-1)$$

is given by

$$v_{OUT}(t) = \sum_{\substack{k=n \\ (k-n \text{ even})}}^{\infty} \frac{\alpha_k \Gamma(k+1) V^k(t) \cos[n\omega_c t + n\phi(t)]}{2^k \Gamma(\frac{k-n}{2} + 1) \Gamma(\frac{k+n}{2} + 1)} \quad (A-2)$$

where $v_{IN}(t) = V(t) \cos \omega_c t + \phi(t)$. (A-3)

Thus the principal envelope term at the n-th harmonic is (k=n in sum)

$$e(t) = \frac{\alpha_n V^n(t)}{2^n}, \quad (A-4)$$

and it is corrupted by the higher order terms (k = n+2, n+3, ...)

$$e(t) = \frac{(n+2)}{2^{n+2}} \alpha_{n+2} V^{n+2}(t) + \frac{(n+4)(n+3)}{2^{n+5}} \alpha_{n+4} V^{n+4}(t) + \\ + \frac{(n+6)(n+5)(n+4)}{(2^{n+7})(3)} \alpha_{n+6} V^{n+6}(t) + \dots \quad (A-5)$$

Assuming that the corrupting terms are uniformly convergent, the principal corrupting term is

$$\epsilon_1(t) = \frac{(n+2)}{2^{n+2}} \alpha_{n+2} V^{n+2}(t) \quad (A-6)$$

A2.0 ACHIEVABLE CANCELLATION IN TERMS OF NONLINEARITY EXPANSION COEFFICIENTS

Let us model the cancellation problem as shown in Figure A-1. We want to find the achievable cancellation ratio as a function of the power series expansion coefficients for the two nonlinearities, $\{\alpha_i\}$ and $\{\beta_i\}$. Based on Section A1, we will model the envelopes at the n -th harmonic, $v_{1,n}(t)$ and $v_{2,n}(t)$, as the sum of their principal terms plus their principal corrupting terms,

$$\begin{aligned} v_{1,n}(t) &\approx \frac{v^n(t)}{2^n} \alpha_n + \frac{(n+2)}{4} \alpha_{n+2} v^2(t) \\ v_{2,n}(t) &\approx \frac{v^n(t)}{2^n} \beta_n + \frac{(n+2)}{4} \beta_{n+2} v^2(t) \end{aligned} \quad (\text{A-7})$$

The output residue power from a cancellation system such as that shown in Figure A-1 is

$$|\epsilon|^2 = \int |V_1(\omega) - WV_2(\omega)|^2 d\omega$$

where $V_1(\omega)$ and $V_2(\omega)$ are the Fourier transforms of $v_1(t)$ and $v_2(t)$ and W is a complex-valued weight. The residue $|\epsilon|^2$ is minimized when W is selected such that

$$\int [V_1(\omega) - WV_2(\omega)] V_2^*(\omega) d\omega = 0$$

giving

$$W = \frac{\int V_1(\omega) V_2^*(\omega) d\omega}{\int |V_2(\omega)|^2 d\omega}$$

Using this, $|\epsilon|^2$ becomes

$$|\epsilon|^2 = \int |V_1(\omega)|^2 d\omega - \frac{\int |V_1(\omega) V_2^*(\omega)|^2 d\omega}{\int |V_2(\omega)|^2 d\omega}$$

Normalizing this by the power in the unweighted channel yields the cancellation ratio

$$\begin{aligned} \text{CR} &= \frac{|\epsilon|^2}{\int |V_1(\omega)|^2 d\omega} \\ &= 1 - \frac{\int |V_1(\omega) V_2^*(\omega)|^2 d\omega}{\int |V_1(\omega)|^2 d\omega \int |V_2(\omega)|^2 d\omega} \end{aligned}$$

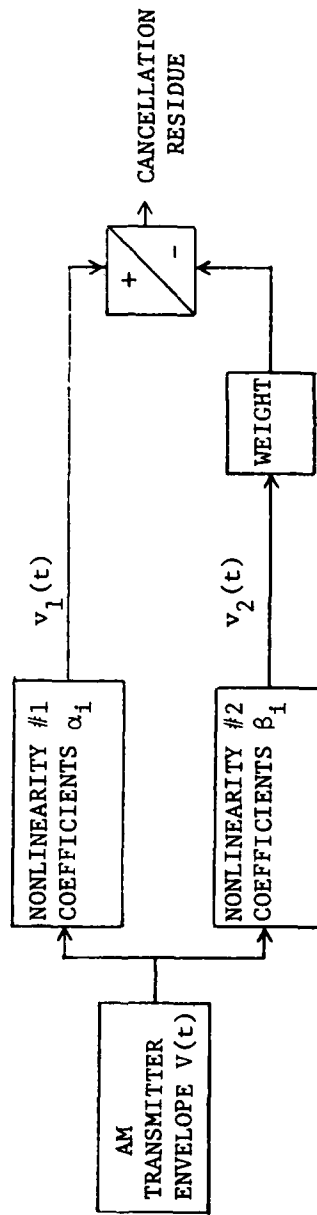


FIGURE A-1. MODEL FOR CANCELLATION ANALYSIS

Applying Parseval' Theorem and retaining only the envelope terms yields the optimum cancellation ratio

$$CR = 1 - \frac{[\int v_1(t)v_2(t)dt]^2}{\int v_1^2(t)dt \int v_2^2(t)dt} \quad (A-8)$$

where CR is the numerical ratio of the output power to power at the unweighted input. Inserting (A-7) into (A-8) gives

$$\begin{aligned} CR &= 1 - \frac{\{\int [\alpha_n v^n(t) + \frac{n+2}{4} \alpha_{n+2} v^{n+2}(t)] [\beta_n v^n(t) + \frac{n+2}{4} \beta_{n+2} v^{n+2}(t)] dt\}^2}{\int [\alpha_n v^n(t) + \frac{n+2}{4} \alpha_{n+2} v^{n+2}(t)]^2 dt \int [\beta_n v^n(t) + \frac{(n+2)}{4} \beta_{n+2} v^{n+2}(t)]^2 dt} \\ &= 1 - \frac{\{\int [\alpha_n \beta_n v^{2n}(t) + \frac{(n+2)}{4} (\alpha_n \beta_{n+2} + \beta_n \alpha_{n+2}) v^{2n+2}(t) + \frac{(n+2)^2}{16} \alpha_{n+2} \beta_{n+2} v^{2n+4}(t)] dt\}^2}{\int [\alpha_n^2 v^{2n}(t) + \alpha_n \alpha_{n+2} \frac{(n+2)}{2} v^{2n+2}(t) + \frac{(n+2)^2}{16} \alpha_{n+2}^2 v^{2n+4}(t)] dt \cdot} \\ &\quad \cdot \int [\beta_n^2 v^{2n}(t) + \beta_n \beta_{n+2} \frac{(n+2)}{2} v^{2n+2}(t) + \frac{(n+2)^2}{16} \beta_{n+2}^2 v^{2n+4}(t)] dt \end{aligned} \quad (A-9)$$

As a worst case let us consider the AM transmitter to be sinusoidally modulated, double sideband suppressed carrier. This is chosen as a worst case because the envelope covers the full range between its peak value and zero, and because it spends a large percentage of its time near its peak value where the harmonics generated are strongest. Thus, we write

$$V(t) = A \cos \omega_m t \quad (A-10)$$

The evaluation of the integrals in (9) is straightforward, resulting in the following

$$\begin{aligned} \int v^{2n}(t) dt &= \frac{A^{2n}}{2^{2n}} \binom{2n}{n} \\ \int v^{2n+2}(t) dt &= \frac{A^{2n+2}}{2^{2n+2}} \binom{2n+2}{n+1} = \frac{A^2 (2n+1)}{2(n+1)} \cdot \frac{A^{2n}}{2^{2n}} \binom{2n}{n} \\ \int v^{2n+4}(t) dt &= \frac{A^{2n+4}}{2^{2n+4}} \binom{2n+4}{n+2} = \frac{A^4 (2n+1)(2n+3)}{4(n+1)(n+2)} \cdot \frac{A^{2n}}{2^{2n}} \binom{2n}{n} \end{aligned} \quad (A-11)$$

where the notation $\binom{k}{j}$ is the binomial coefficient

$$\binom{k}{j} = \frac{k!}{j!(k-j)!} \quad (\text{A-12})$$

Inserting (11) into (9) gives

$$\begin{aligned} \text{CR} = 1 - \frac{\{\alpha_n \beta_n + \frac{(n+2)}{4} [\frac{A^2(2n+1)}{2(n+1)}] (\alpha_n \beta_{n+2} + \beta_n \alpha_{n+2}) + \frac{(n+2)^2}{16} [\frac{A^4(2n+1)(2n+3)}{4(n+1)(n+2)}] \cdot \alpha_{n+2} \beta_{n+2}\}^2}{\{\alpha_n^2 + \alpha_n \alpha_{n+2} \frac{(n+2)}{2} [\frac{A^2(2n+1)}{2(n+1)}] + \frac{(n+2)^2}{16} \alpha_{n+2}^2 [\frac{A^4(2n+1)(2n+3)}{4(n+1)(n+2)}]\} \cdot \{\beta_n^2 + \beta_n \beta_{n+2} \frac{(n+2)}{2} [\frac{A^2(2n+1)}{2(n+1)}] + \frac{(n+2)^2}{16} \beta_{n+2}^2 [\frac{A^4(2n+1)(2n+3)}{4(n+1)(n+2)}]\}} \quad (\text{A-13}) \end{aligned}$$

Collecting terms in (13) over a common denominator results in

$$\begin{aligned} \text{CR} = \frac{A^4 (\alpha_n \beta_{n+2} - \beta_n \alpha_{n+2})^2 (n+2)(2n+1)}{64(n+1)^2 \left\{ \alpha_n^2 + \frac{\alpha_n \alpha_{n+2} A^2 (n+2)(2n+1)}{4(n+1)} + \frac{\alpha_{n+2}^2 A^4 (n+2)(2n+1)(2n+3)}{64(n+1)} \right\} \cdot \left\{ \beta_n^2 + \frac{\beta_n \beta_{n+2} A^2 (n+2)(2n+1)}{4(n+1)} + \frac{\beta_{n+2}^2 A^4 (n+2)(2n+1)(2n+3)}{64(n+1)} \right\}} \quad (\text{A-14}) \end{aligned}$$

Dividing numerator and denominator by $\alpha_n^2 \beta_n^2$ and dropping higher order terms results in

$$\begin{aligned} \text{CR} \approx \frac{A^4 \frac{\beta_{n+2}}{\beta_n} - \frac{\alpha_{n+2}}{\alpha_n} \frac{A^2 (n+2)(2n+1)}{4(n+1)}}{64(n+1)^2 \left\{ 1 + \frac{\alpha_{n+2}}{\alpha_n} \cdot \frac{A^2 (n+2)(2n+1)}{4(n+1)} \right\} \cdot \left\{ 1 + \frac{\beta_{n+2}}{\beta_n} \cdot \frac{A^2 (n+2)(2n+1)}{4(n+1)} \right\}} \quad (\text{A-15}) \end{aligned}$$

Note that if the nonlinearities are identical, the numerator, and hence the CR, go to zero, implying perfect cancellation.

A3.0 ACHIEVABLE CANCELLATION RATIO IN TERMS OF MEASURABLE HARMONIC POWER LEVELS

The coefficients $\{\alpha_n\}$ and $\{\beta_n\}$ are not easily measured directly, and hence the utility of Equation (A-15) is less than ideal. However, these coefficients may be directly related to the power measurements made at the individual harmonics with the same AM fundamental to provide a more useful result.

We approximate the power levels at the n-th harmonic of each non-linearity, by using only the first term of (A-7) to obtain

$$\begin{aligned} P_{1,n} &= \int v_{1,n}^2(t) dt \approx \left(\frac{\alpha_n}{2^n}\right)^2 \int v^{2n}(t) dt \\ P_{2,n} &= \int v_{2,n}^2(t) dt \approx \left(\frac{\beta_n}{2^n}\right)^2 \int v^{2n}(t) dt \end{aligned} \quad (A-16)$$

Performing the integrations with $V(t)$ given by (A-10), we obtain

$$\begin{aligned} P_{1,n} &\approx \frac{\alpha_n^2 A^{2n}}{2^{4n}} \binom{2n}{n} \\ P_{2,n} &\approx \frac{\beta_n^2 A^{2n}}{2^{4n}} \binom{2n}{n} \end{aligned} \quad (A-17)$$

Likewise, the power levels at the (n+2)-th harmonics are given by

$$\begin{aligned} P_{1,n+2} &\approx \frac{\alpha_{n+2}^2 A^{2(n+2)}}{2^{4(n+2)}} \binom{2n+4}{n+2} \\ P_{2,n+2} &\approx \frac{\beta_{n+2}^2 A^{2(n+2)}}{2^{4(n+2)}} \binom{2n+4}{n+2} \end{aligned} \quad (A-18)$$

The ratios of the corresponding expressions in (A-17) and (A-18) is

$$\begin{aligned} \frac{P_{1,n+2}}{P_{1,n}} &\approx \left(\frac{\alpha_{n+2}}{\alpha_n}\right)^2 \frac{A^4}{2^8} \frac{\binom{2n+4}{n+2}}{\binom{2n}{n}} = \left(\frac{\alpha_{n+2}}{\alpha_n}\right)^2 \frac{A^4}{2^6} \frac{(2n+1)(2n+3)}{(n+1)(n+2)} \\ \frac{P_{2,n+2}}{P_{2,n}} &\approx \left(\frac{\beta_{n+2}}{\beta_n}\right)^2 \frac{A^4}{2^6} \frac{(2n+1)(2n+3)}{(n+1)(n+2)} \end{aligned} \quad (A-19)$$

whence

$$\frac{\alpha_{n+2} A^2}{\alpha_n} = 2^3 \sqrt{\frac{P_{1,n+2}(n+1)(n+2)}{P_{1,n}(2n+1)(2n+3)}} \quad (A-20)$$

$$\frac{\beta_{n+2} A^2}{\beta_n} = 2^3 \sqrt{\frac{P_{2,n+2}(n+1)(n+2)}{P_{2,n}(2n+1)(2n+3)}}$$

We now insert

$$CR \approx \frac{(n+2)^2 (\sqrt{P_{2,n+2}/P_{2,n}} - \sqrt{P_{1,n+2}/P_{1,n}})^2}{(n+1)(2n+3) \{1 + 2\sqrt{P_{1,n+2}/P_{1,n}} \cdot [(n+2)^3(2n+1)/(n+1)(2n+3)]\} \cdot \{1 + 2\sqrt{P_{2,n+2}/P_{2,n}} \cdot [(n+2)^3(2n+1)/(n+1)(2n+3)]\}} \quad (A-21)$$

For large n , we can further simplify (A-21) to obtain

$$CR \approx \frac{(\sqrt{P_{2,n+2}/P_{2,n}} - \sqrt{P_{1,n+2}/P_{1,n}})^2}{2\{1+2n\sqrt{P_{1,n+2}/P_{1,n}}\}\{1+2n\sqrt{P_{2,n+2}/P_{2,n}}\}}, \text{ for } n \geq 5. \quad (A-22)$$

3.1 EVALUATION FOR SOME SPECIAL CASES

Equation (22) will be evaluated for two cases.

Case 1: Rapid decrease in harmonic energy.

Suppose $2n\sqrt{P_{1,n+2}/P_{1,n}} < 1$ and $2n\sqrt{P_{2,n+2}/P_{2,n}} < 1$. Then

$$\sqrt{P_{2,n+2}/P_{2,n}} - \sqrt{P_{1,n+2}/P_{1,n}} < 1/2n$$

and

$$CR < \frac{1}{2} \left(\frac{1}{2n}\right)^2$$

as an upper bound.

Case 2: Slow decrease in harmonic energy.

Suppose $2n\sqrt{P_{1,n+2}/P_{1,n}} > 1$ and $2n\sqrt{P_{2,n+2}/P_{2,n}} > 1$. Then

$$CR \approx \frac{1}{8n^2} (\sqrt{P_{1,n}/P_{1,n+2}} - \sqrt{P_{2,n}/P_{2,n+2}})^2$$

whence we can upper-bound CR as

$$CR < 1/2.$$

These results lend credence to the intuitive conclusion that where the harmonic power levels decrease slowly, the achievable cancellation ratio is much more dependent on matching of the nonlinearities. Case 1 above corresponds to the situation where the harmonic level falls off rapidly. Case 2 corresponds to the situation where the harmonic level does not decay as rapidly, thereby leading to a smaller cancellation ratio as shown by the upper bound found above.

APPENDIX B
LISTING OF FORTRAN PROGRAM

This appendix contains a listing of the FORTRAN program which simulates the key portions of an harmonic cancellation system.

```

C          HARMONICS CANCELLATION
5017      FORMAT(2X,'SIMUL PROG: NLND1      FUND: AI/SC ')
          DIMENSION A(10),IRW(2100)
          1,IQW(2100),ALER(10),ALHR(10)
          COMPLEX CVO,CVU,CERR,CIW,CSSH,CV

C
          TI=2.5
          NG=11
          FS=10000.
          G=1.0
          FO=1217.
1          TYPE 5011, TI, NG, FS, G, FO
5011      FORMAT(2X,'RUN TIME(1)=' ,F10.4,'      NUM ADDR BITS(2)=' ,14,
          1 /,2X,'SAMPLE RATE(3)=' ,F9.0,'      GAIN(4)=' ,F10.3,
          2 /,2X,'FUND FREQ(5)='F9.0)
          TYPE 5013
5013      FORMAT(2X,'ENTER DESIRED CHANGE: NUM AND VALUE')
          ACCEPT *,ICNG,VAL
          ICNG=ICNG+1
          GO TO (70,10,15,20,25,30) ICNG
10         TI=VAL
          GO TO 1
15         NG=VAL
          GO TO 1
20         FS=VAL
          GO TO 1
25         G=VAL
          GO TO 1
30         FO=VAL
          GO TO 1
70         CALL ASSIGN (6,9HRSXNL.DAT,9,, 'CC')
5007      FORMAT (2X,'SAMPL RATE = ' ,F9.0,3X,'NUM ADDR BITS=' ,14,3X,
          1 'GAIN=' ,F10.3)
5009      FORMAT (2X,'FUND FREQ=' ,F9.0,3X,'RUN TIME=' ,F10.4,3X)
          TYPE 5017
          PRINT 5017
          PRINT 5007, FS,NG,G
          PRINT 5009, FO,TI
          DO 150 1A=1,2100
          IRW(1A)=0
          IQW(1A)=0
150       CONTINUE
          N=3
          PI=3.14159
          PI2=PI/2.
          PI4=PI/4.
          PI43=3.*PI4
          ERSQS=0.0
          HRSQS=0.0
          K=1
          WO=2.*PI*FO

```

```

JP=0
DELT=1/FS
T=DELT
100 FLIM=2.0**NG-1.0
CONTINUE
AVO=0.98*SIN(WO*T)
ANGH=PI4
IF(AVO.LT.0.) ANGH = -PI43
CVO=CMPLX(AVO,0.0)
C
AVH=AVC**2
AVHH=1 +(AVH/4.)*(1.+(AVH*.1)*(1.+AVH/18.))
AVHH=0.77563*AVHH*AVH*AVO
AVHB=0.98*AVO**5
CVH=CMPLX(AVHH,AVHB)
C
CVO=FLIM*CVO
CVH=FLIM*CVH
ACVO=CABS(CVO)
RCCSH=COS(ANGH)
QCCSH=SIN(ANGH)
CCSH=1.414*CMPLX(RCCSH,QCCSH)
IF(ACVO.GE.FLIM) ACVO=(FLIM)
IA=IFIX(ACVO)+1
RSH=FLOAT(IRW(IA))*REAL(CCSH)
QSH=FLOAT(IQW(IA))*AIMAG(CCSH)
RERR=-REAL(CVH)+RSH
QERR=-AIMAG(CVH)+QSH
RCER=-G*RERR*SIGN(1.,RCCSH)
QCER=-G*QERR*SIGN(1.,QCCSH)
IF(RCER.GE.FLIM) RCER=FLIM
IF(RCER.LE.-FLIM) RCER=-FLIM
IF(QCER.GE.FLIM) QCER=FLIM
IF(QCER.LE.-FLIM) QCER=-FLIM
IQCER=IFIX(QCER)
IRCER=IFIX(RCER)
IRW(IA)=IRW(IA)+IRCER
IQW(IA)=IQW(IA)+IQCER
IF(IRW(IA).GE.FLIM) IRW(IA)=FLIM
IF(IRW(IA).LE.-FLIM) IRW(IA)=-FLIM
IF(IQW(IA).GE.FLIM) IQW(IA)=FLIM
IF(IQW(IA).LE.-FLIM) IQW(IA)=-FLIM
ERSQ=RERR**2+QERR**2
HRSQ=(REAL(CVH))**2+(AIMAG(CVH))**2
ERSQS=ERSQS+ERSQ
HRSQS=HRSQS+HRSQ
IF(K.EQ.100) GO TO 300
K=K+1
GO TO 250

```

```

300      K=1
        AER=ERSQS/HRSQS
        AHR=HRSQS/100.0
        ERSQS=0.0
        HRSQS=0.0
        IF(AER.LT.1E-9) AER=1E-9
        IF(AHR.LT.1E-9) AHR=1E-9
        JP=MOD(JP,10)+1
        ALER(JP)=10*ALOG10(AER)
        ALHR(JP)=10*ALOG10(AHR)
        IF(JP.NE.10) GO TO 250
        TYPE 222,ALER,T,ALHR
        PRINT 222,ALER,T,ALHR
222     FORMAT(4X,10(F6.1,1X),2X,F7.5/4X,10(F6.1,1X))
250     CONTINUE
255     T=DELT+T
        IF(T.GT.T1) GO TO 999
        GO TO 100
999     CONTINUE
        IMAX=-14000
        IMIN=14000
        DO 650 J=1,2100
        IMAX=MAX0(IMAX,IRW(J),IQW(J))
650     IMIN=MIN0(IMIN,IRW(J),IQW(J))
        MIMIN=IABS(IMIN)
        IMAX=MAX0(MIMIN,IMAX)
        PRINT 5021,IMAX
        TYPE 5021,IMAX
5021    FORMAT(2X,'MAX MEM VALUE = ',I10)
        TYPE 5000
5000    FORMAT(2X,'ENTER 1 FOR COMPLEX WEIGHT PLOT...')
        ACCEPT 5001,IPL0T
5001    FORMAT (I1)
        IF(IPL0T.NE.1) GO TO 1100
        FSCLF=230.0/IMAX
        DO 675 KA=4,2100,4
        J=KA/4
675     IRW(J)=IRW(KA)*FSCLF
        DO 690 L=4,2100,16
        JA=L/4
        IQW(JA)=IQW(L)*FSCLF
        LA=L+4
        IQW(JA+1)=IQW(LA)*FSCLF
        IQW(JA+2)=0

```



```
590    IQW(JA+3)=0
      CALL PLOT55(9,0,0)
      CALL PLOT55(10,,)
      CALL PLOT55(2,1+2+4+32+64+512,)
      CALL PLOT55(7,0,0)
      CALL PLOT55(1,0,)
      IX=0
      IY=0
      DO 700 J=1,11
      CALL PLOT55(5,IX,1)
      CALL PLOT55(4.1,IY)
      IX=IX+50
      IY=IY+23
700    CONTINUE
      CALL PLOT55(3,-512,IRW)
      CALL PLOT55(1,1,)
      CALL PLOT55(3,-512,IQW)
      READ(5,5003)
5003   FORMAT(I5)
      CALL PLOT55(2,1+2+4+32+64+512,)
      CALL PLOT55(2,512,)
      CALL PLOT55(9,0,0)
      CALL PLOT55(10,,)
      CALL PLOT55(2,,1+2+4+32+64+512)
1100   END
```

REFERENCES

- [1] "Nonlinear Interference Cancellation System," RADC-TR-78-225, November 1978, B032512L.
- [2] Higa, Walter H., "Spurious Signals Generated by Electron Tunneling on Large Reflector Antennas," Proc IEEE, vol. 63, no. 2, February 1975.
- [3] Chase, W.M., J.W. Rockway and G.C. Salisbury, "A Method of Detecting Significant Sources of Intermodulation Interference," IEEE Trans on Electromagnetic Compatibility, vol. EMC-17, no. 2, May 1975.
- [4] Chase, W.M., "Ship RFI Survey Procedure for HF Frequencies," NELC Technical Document 336, 21 June 1974.
- [5] Wiener, N. Nonlinear Problems in Random Theory, MIT Press, 1958.
- [6] "Nonlinearity System Modelling and Analysis with Application to Communication Receivers," RADC TR-73-178, June 1978, 766278/6.
- [7] Thomas, E.J., "An Adaptive Echo Canceller in a Nonideal Environment (Nonlinear or Time Variant)," BSTJ, vol. 50, no. 8, October 1971.
- [8] Falconer, D.D., "Adaptive Equalization of Channel Nonlinearities in QAM Data Transmission Systems," BSTJ, vol. 57, no. 7, September 1978.
- [9] Davenport, W.B., Root, W.L., An Introduction to the Theory of Random Signals and Noise, McGraw-Hill Book Co., New York, 1978, p. 284.
- [10] Jolley, B.W., Summation of Series, Dover Press, 1961.
- [11] M. Schetzen, "Determination of Optimum Nonlinear Systems for Generalized Error Criteria Based on the Use of Gate Functions," IEEE Trans on Information Theory, January 1965, pp. 117-125.

MISSION
of
Rome Air Development Center

RADC plans and executes research, development, test and selected acquisition programs in support of Command, Control Communications and Intelligence (C³I) activities. Technical and engineering support within areas of technical competence is provided to ESD Program Offices (POs) and other ESD elements. The principal technical mission areas are communications, electromagnetic guidance and control, surveillance of ground and aerospace objects, intelligence data collection and handling, information system technology, ionospheric propagation, solid state sciences, microwave physics and electronic reliability, maintainability and compatibility.

**DATE
FILMED**
2-8